Received: 25 September 2021 | Revised: 17 April 2022 | Accepted: 16 June 2022

DOI: 10.1002/rnc.6258

RESEARCH ARTICLE

WILEY

Tracking control for large-scale switched nonlinear systems subject to asymmetric input saturation and output hysteresis: A new adaptive network-based approach

Yu-Qun Han[1,2] | **Wen-Jing He**[1] | **Na Li**[1] | **Shan-Liang Zhu**[1,2]

[1]School of Mathematics and Physics, Qingdao University of Science and Technology, Qingdao, China

[2]Research Institute for Mathematics and Interdisciplinary Sciences, Qingdao University of Science and Technology, Qingdao, China

Correspondence
Shan-Liang Zhu, School of Mathematics and Physics, Qingdao University of Science and Technology, Qingdao 266061, China.
Email: zhushanliang@qust.edu.cn

Funding information
Natural Science Foundation of Shandong Province, Grant/Award Number: ZR2020QF055

Abstract

For large-scale switched nonlinear systems subject to asymmetric input saturation and output hysteresis, an adaptive control strategy is put forward by using a novel neural network, that is, multi-dimensional Taylor network (MTN), which can effectively cope with the output tracking problem of this system. Firstly, asymmetric input saturation is expressed as the combination of a linear function and a bounded error function. Then, the modified Bouc-Wen hysteresis model is employed to solve the nonlinear problem caused by output hysteresis. Afterwards, based on the approximation ability of MTN, a novel adaptive decentralized control method is designed by combining Lyapunov stability theory with adaptive backstepping technology, which realizes the stability and boundedness of the controlled systems. It should be noted that the asymmetric input saturation, the output hysteresis, large-scale nonlinear systems and switched nonlinear systems appear in the same framework for the first time. Finally, a practical example and a numerical example are given to verify the availability of the proposed control strategy.

KEYWORDS

asymmetric input saturation, large-scale nonlinear systems, multi-dimensional Taylor network, output hysteresis, switched nonlinear systems

1 | INTRODUCTION

Of late years, the control of nonlinear systems subject to uncertain structures has fascinating serious attention in the field of automation control.[1-3] As two kinds of general approximators, fuzzy logic systems (FLSs) and neural networks (NNs) are used to cope with the uncertainty problems caused by unknown nonlinear structures in the systems.[4-8] Among them, multi-dimensional Taylor network (MTN), as a novel kind of NN, has been utilized to a host of nonlinear systems due to its simple structure and powerful approximation performance, such as large-scale systems,[9,10] switched systems,[11] stochastic systems[12,13] and discrete-time systems.[14] Unfortunately, so far, it is complete blank to fulfill the research on the control of large-scale switched nonlinear systems via the MTN technology.

As the combination of interrelated subsystems, large-scale systems are comprehensively utilized in practical systems, including multi-agent systems,[15] aerospace systems[16] and power systems.[17] Therefore, the research on control and dynamic modeling of large-scale systems is of great practical significance. However, the control design of large-scale systems has become a significantly challenging problem due to the dispersion of controlled objects and the large number

of variables. In order to solve this control problem, great deals of adaptive decentralized control approaches have been published.[18-20] Among them, on the basis of large-scale systems, switched systems, as a significant class of hybrid systems with the unified dynamic mathematical model, have a profound industrial application background.[21,22] Consequently, it is a great value to investigate decentralized control of large-scale switched nonlinear systems. Therefore, for large-scale switched nonlinear systems, quite a lot adaptive decentralized control strategies based on backstepping have been published.[23,24] However, it should be pointed out that the control design and stability analysis of large-scale switched nonlinear systems are complex due to the fact that the interactions of various inputs and outputs. Especially for the constraints analysis of various inputs and outputs, how to cope with the input and output constraints problem for large-scale switched nonlinear systems turns into a serious challenge.

On the one hand, the problem of input saturation is inevitable in a multitude of practical dynamic systems. Input saturation restricts the size of the control signals in the system and severely affects the stability of the system, which in turn decreases the control accuracy. Therefore, for the sake of dealing with the input saturation problems in large-scale systems or switched systems, lots of control strategies have been proposed.[25-29] The authors of Reference 26 discussed the control issue of large-scale Markovian jump nonlinear systems with input saturation, but only the symmetric saturation constraint was considered. However, it is also extraordinarily crucial and quite challenging to consider asymmetric input constraints for nonlinear systems. On the other hand, hysteresis often occurs in the field of realistic systems.[30,31] The nonlinear problem depends not only on input but also on output, which is caused by hysteresis. Therefore, the research on hysteresis has become a characteristic challenge in the control systems. For the sake of solving this challenge, quite a lot of mathematical models have been proposed, such as PI model,[32] hysteresis inverse model[33] and Duhen model.[34] Compared with the above models, the modified Bouc-Wen hysteresis model was put forward by,[35] which can preferably solve the more general hysteresis problem. Based on the modified Bouc-Wen hysteresis model, for switched systems or large-scale systems, many interesting research results about unknown hysteresis have been obtained, such as input hysteresis,[36,37] backlash-like hysteresis,[38] output hysteresis[39,40]. However, according to our current knowledge, there is no research on large-scale switched nonlinear systems with output hysteresis. Based on the above discussion, it is more important and sense that how to compensate the influence of asymmetric input saturation constraint and output hysteresis constraint has become an urgent problem for large-scale switched nonlinear systems.

In this article, the tracking control problem for large-scale switched systems subject to asymmetric input saturation and output hysteresis is discussed. Firstly, the asymmetric input saturation is transformed into the combination of a linear function and a bounded error function. Then, the modified Bouc-Wen hysteresis model is applied to solve the nonlinear problem caused by output hysteresis. Finally, an adaptive MTN-based control strategy is put forward, which combines adaptive control and decentralized control in backstepping control process. The results show that the proposed control strategy is effective. Compared with the existing literatures, the major contributions of this article are as follows:

(1) As a special NN, MTN is utilized on large-scale switched nonlinear systems for the first time. Based on the same MTN estimation technology, the control scheme proposed in this article has quite differences from References 9-12. Unlike,[9,10] the control issue of switched nonlinear systems is effectively solved. Different from Reference 11 and 12, decentralized control research of large-scale systems is involved.
(2) It is the first time that, as a class of nonlinear constraints, asymmetric input saturation is considered in large-scale switched nonlinear systems. Although the tracking control problem of large-scale switched systems subject to input saturation was researched by,[26] only the symmetric input saturation constraint was considered. The asymmetric input saturation constraints were considered in References 27-29, but these studies cannot cope with the control problems of large-scale switched nonlinear systems.
(3) According to our current knowledge, there is no research on large-scale nonlinear systems subject to output hysteresis. In this article, the modified Bouc-Wen hysteresis model proposed by Zhou et al.[35] to cope with the input hysteresis issue is extended to the output hysteresis, and which is applied to large-scale switched nonlinear systems. The control strategy proposed in Reference 36 is only suitable for controlling large-scale systems with unknown actuator hysteresis, rather than switched systems with output hysteresis. Even though the control results of switched systems with output hysteresis were reported in References 39 and 40, the controlled objects do not include large-scale systems. The authors of References 23 and 24 considered the tracking control problem of large-scale switched systems, but the problem of output hysteresis cannot be solved.
(4) It seems to us that little has been known about the research of large-scale systems, switched systems, asymmetric input saturation, output hysteresis and MTN technology appearing in the same framework.

2 | PRELIMINARIES AND FORMULATION

2.1 | System description

Considering a class of large-scale switched nonlinear systems subject to asymmetric input saturation and output hysteresis, which consists of N subsystems.

$$\begin{cases} \dot{\phi}_{i,j} = \phi_{i,j+1} + \gamma_{i,j,\sigma(t)}\left(\overline{\boldsymbol{\phi}}_{i,j}\right) + \Delta_{i,j,\sigma(t)}\left(t, \overline{\boldsymbol{\phi}}_{i,j}\right) + A_{i,j,\sigma(t)}(\overline{\boldsymbol{y}}) \\ \dot{\phi}_{i,n_i} = u_i(v_i) + \gamma_{i,n_i,\sigma(t)}\left(\overline{\boldsymbol{\phi}}_{i,n_i}\right) + \Delta_{i,n_i,\sigma(t)}\left(t, \overline{\boldsymbol{\phi}}_{i,n_i}\right) + A_{i,n_i,\sigma(t)}(\overline{\boldsymbol{y}}) \\ y_i = \Xi_i\left(\phi_{i,1}\right) \end{cases} \tag{1}$$

in system (1), i and j satisfy $i = 1, \ldots, N, j = 1, 2, \ldots, n_i - 1$, respectively. In addition, $\phi_{i,j}$ mean the states of the i th system and $\overline{\boldsymbol{\phi}}_{i,j} = \left[\phi_{i,1}, \phi_{i,2}, \ldots, \phi_{i,j}\right]^{\mathrm{T}} \in R^j, \overline{\boldsymbol{\phi}}_{i,n_i} = \left[\phi_{i,1}, \phi_{i,2}, \ldots, \phi_{i,n_i}\right]^{\mathrm{T}} \in R^{n_i}$. $y_i = \Xi_i\left(\phi_{i,1}\right)$ express the output of the i th system with hysteresis and $\overline{\boldsymbol{y}} = [y_1, \ldots, y_N]^{\mathrm{T}} \in R^N$. $\sigma(t) : R_+ \to M = \{1, 2, \ldots, m\}$ represents the switching signal and m denotes the number of subsystem. With regard to $\forall k \in M, j = 1, \ldots, n_i, \gamma_{i,j,k}\left(\overline{\boldsymbol{\phi}}_{i,j}\right)$ show the unknown nonlinear smooth functions, and $\Delta_{i,j,k}\left(t, \overline{\boldsymbol{\phi}}_{i,j}\right)$ show the unknown time-varying disturbance, and $A_{i,j,k}(\overline{\boldsymbol{y}})$ indicate the interconnections between subsystems. v_i, u_i are the input and output of asymmetric nonsmooth saturation nonlinearity in the i th system, respectively. $u_i(v_i)$ can be expressed as

$$u_i(v_i) = \begin{cases} H_{i,\max}, v_i \geq u_{i,\max} \\ h_i(v_i), -u_{i,\min} \leq v_i < u_{i,\max} \\ -H_{i,\min}, v_i < -u_{i,\min} \end{cases}, \tag{2}$$

where $u_{i,\max}, u_{i,\min} > 0$ define the break points. $H_{i,\max}, H_{i,\min} > 0$ are the bounds of $u_i(v_i)$. $h_i(v_i)$ are the unknown smooth and continuous nonlinear functions. $u_i(v_i)$ represent the asymmetric input saturation constraint regarded in this article, which are displayed in Figure 1.

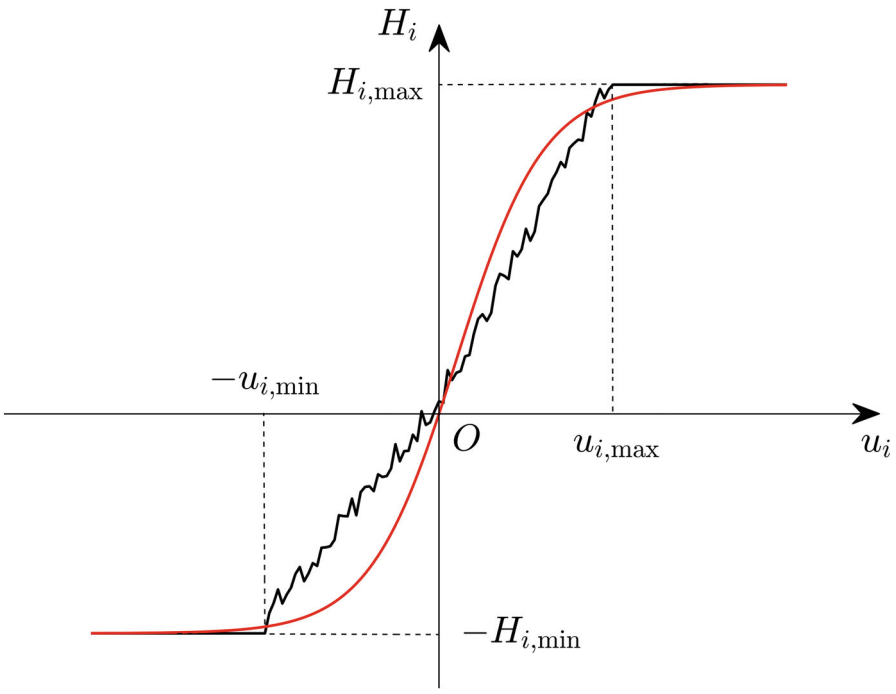

FIGURE 1 Asymmetric input saturation constraint

The objectives of the control scheme proposed in this article for system (1) are as follows:

(i) For the closed-loop system, all signals in it are bounded;
(ii) For the reference signals $y_{i,d}$, the tracking error $y_i - y_{i,d}$ can be adjusted near the origin.

Assumption 1 (11). For $\forall t \geq 0$, $i = 1, 2, \ldots, N$ and $\underset{-}{Y}_{i,0}, \overline{Y}_{i,0}, Y_{i,1}, \ldots, Y_{i,n} > 0$ are constants, the $y_{i,d}$ and their time derivative $y_{i,d}^{(j)}, j = 1, 2, \ldots, n$ satisfy the inequalities as follows $-\underset{-}{Y}_{i,0} \leq y_{i,d}(t) \leq \overline{Y}_{i,0}, \left|\dot{y}_{i,d}(t)\right| < Y_{i,1}, \ldots, \left|y_{i,d}^{(n)}(t)\right| < Y_{i,n}$.

Assumption 2 (39). For $\forall k \in M$, $i = 1, 2, \ldots, N$ and $j = 1, 2, \ldots, n_i$, the time-varying disturbance $\Delta_{i,j,k}\left(t, \overline{\boldsymbol{\phi}}_{i,j}\right)$ satisfy the following conditions.

$$\Delta_{i,j,k}\left(t, \overline{\boldsymbol{\phi}}_{i,j}\right) \leq \varphi_{i,j,k}\left(t, \overline{\boldsymbol{\phi}}_{i,j}\right) + \tilde{\varphi}_{i,j,k} \tag{3}$$

where $\varphi_{i,j,k}\left(t, \overline{\boldsymbol{\phi}}_{i,j}\right)$ are unknown continuous functions and $\tilde{\varphi}_{i,j,k} > 0$ are constants.

Remark 1. The main idea of (3) is derived from Reference 41. With the aim of handling the discontinuous and unknown time-varying disturbance $\Delta_{i,j,k}\left(t, \overline{\boldsymbol{\phi}}_{i,j}\right)$, continuous functions $\varphi_{i,j,k}\left(t, \overline{\boldsymbol{\phi}}_{i,j}\right)$ and constants $\tilde{\varphi}_{i,j,k}$ are designed. The constants $\tilde{\varphi}_{i,j,k}$ ensure that (3) hold for more general time-varying disturbance.

Assumption 3 (10). Combining with the mean value theorem, it can be obtained that nonlinear functions $A_{i,j,k}(\overline{\boldsymbol{y}})$ satisfy the following conditions

$$\left|A_{i,j,k}(\overline{\boldsymbol{y}})\right|^2 \leq \sum_{l=1}^{N} A_{i,j,k,l}^2(y_l) \leq \sum_{l=1}^{N} y_l^2 \tilde{A}_{i,j,k,l}^2(y_l) \tag{4}$$

with $A_{i,j,k,l}(y_l)$, $\tilde{A}_{i,j,k,l}(y_l)$ express unknown nonlinear functions.

2.2 | Preprocessing of asymmetric input saturation model

For the sake of solving the nonsmooth problem in model (2), similar to Reference 29, continuous functions $\chi_i(v_i)$ are used to approximate $u_i(v_i)$. Then smooth models are obtained as follows

$$\chi_i(v_i) = \begin{cases} u_{i,\max} \tanh\left(v_i \Big/ u_{i,\max}\right), v_i \geq 0 \\ -u_{i,\min} \tanh\left(v_i \Big/ u_{i,\min}\right), v_i < 0 \end{cases} \tag{5}$$

with $\tanh(\cdot)$ represents the hyperbolic tangent function. Then, $u_i(v_i)$ can be rewritten as the combination of linear functions and bounded error functions.

$$u_i(v_i) = \chi_i(v_i) + c_i(v_i), \tag{6}$$

where $|c_i(v_i)| = |u_i(v_i) - \chi_i(v_i)| \leq \max\left\{u_{i,\max}, u_{i,\min}\right\}(1 - \tanh(1)) = \bar{c}_i$ and $\bar{c}_i > 0$ are positive constants. Since $\chi_i(0) = 0$, for $\tilde{v}_i \in (0, v_i)$, the following formulas can be obtained by using the mean-value theorem.

$$\chi_i(v_i) = \chi_i'(\tilde{v}_i) v_i \tag{7}$$

with $\chi_i'(\tilde{v}_i)$ are the derivative of $\tilde{v}_i$.

Assumption 4 (27). For the derivative of $\tilde{v}_i$, there is a known constant k that holds the following inequality.

$$0 \leq k \leq \chi_i'(\tilde{v}_i) < \infty. \tag{8}$$

Remark 2. The input saturation constraint considered in this article is asymmetric and nonlinear, which is more comprehensive than References 25 and 26.

2.3 | Processing of output constraint

In an effort to solve the issue of output hysteresis, the method of Reference 35 is introduced. Specifically, the system output y_i can be expressed by the following Bouc-Wen model.

$$y_i = \Xi_i\left(\phi_{i,1}\right) = p_{i,1}\phi_{i,1} + p_{i,2}\hbar_i, \tag{9}$$

where $i = 1, \ldots, N, p_{i,1}, p_{i,2}$ are unknown constants with the same sign. $\hbar_i$ are auxiliary variables and satisfy the following conditions.

$$\begin{cases} \dot{\hbar}_i = \dot{\phi}_{i,1} h_i\left(\hbar_i, \dot{\phi}_{i,1}\right) \\ \hbar_i\left(t_0\right) = 0 \end{cases} \tag{10}$$

with $h_i\left(\hbar_i, \dot{\phi}_{i,1}\right)$ are defined as

$$h_i\left(\hbar_i, \dot{\phi}_{i,1}\right) = 1 - sign\left(\dot{\phi}_{i,1}\right) \iota_i |\hbar_i|^{K_i - 1}\hbar_i - \lambda_i |\hbar_i|^{K_i}, \tag{11}$$

where ι_i, λ_i, K_i denote the hysteretic parameters of the ith system and meet the requirements of $\iota_i > |\lambda_i|, K_i > 1$.

Therefore, from (9), (10), and (11), it follows that

$$\phi_{i,1} = \Xi^{-1}\left(y_i\right) = \frac{1}{p_{i,1}} y_i - \frac{p_{i,2}}{p_{i,1}}\hbar_{i,1}, \tag{12}$$

where $\dot{\hbar}_{i,1} = \frac{1}{p_{i,2} h_i\left(\hbar_{i,1}, \frac{\dot{y}_i}{p_{i,1}}\right) + p_{i,1}} \dot{y}_i h_i\left(\hbar_{i,1}, \frac{\dot{y}_i}{p_{i,1}}\right)$.

Then, new variables $\kappa_i(t)$ are defined, which satisfy

$$\kappa_i(t) = p_{i,1} + p_{i,2} h_i\left(\hbar_i, \dot{\phi}_{i,1}\right). \tag{13}$$

It is of interest to note that, according to Reference 41, the value range of $\kappa_i(t)$ satisfy $\left[-\overline{\kappa}_i, -\underline{\kappa}_i\right] \cup \left[\underline{\kappa}_i, \overline{\kappa}_i\right]$ with $\underline{\kappa}_i > 0$, $\overline{\kappa}_i > 0$, and satisfy

$$\begin{aligned} \underline{\kappa}_i &= \left|p_{i,1}\right| \\ \overline{\kappa}_i &= \left|p_{i,1}\right| + \left|p_{i,2}\right|\left(1 + \frac{\iota_i}{\iota_i + \lambda_i} + \frac{|\lambda_i|}{\iota_i + \lambda_i}\right). \end{aligned} \tag{14}$$

Remark 3. The output hysteresis, auxiliary variables $\hbar_i$ and hysteresis inverse considered in this article are shown in Figure 2. Output hysteresis exists widely in a variety of industrial applications, such as flexible guided lifting systems, steering systems, floating container cranes systems and piezoceramic actuator systems. Therefore, it is of great practical significance to solve the complex nonlinear problem caused by the output hysteresis.

2.4 | Nussbaum-type function

If the following are true, then the function $N(s)$ is a Nussbaum function.

$$\begin{aligned} \lim_{p\to\pm\infty} \sup \frac{1}{p}\int_0^p N(s)ds = \infty, \\ \lim_{p\to\pm\infty} \inf \frac{1}{p}\int_0^p N(s)ds = -\infty. \end{aligned} \tag{15}$$

It should be pointed that, many functions such as $\eta^2\cos\eta, \eta^2\sin\eta, \exp\left(\eta^2\right)$ satisfy the conditions of (15).

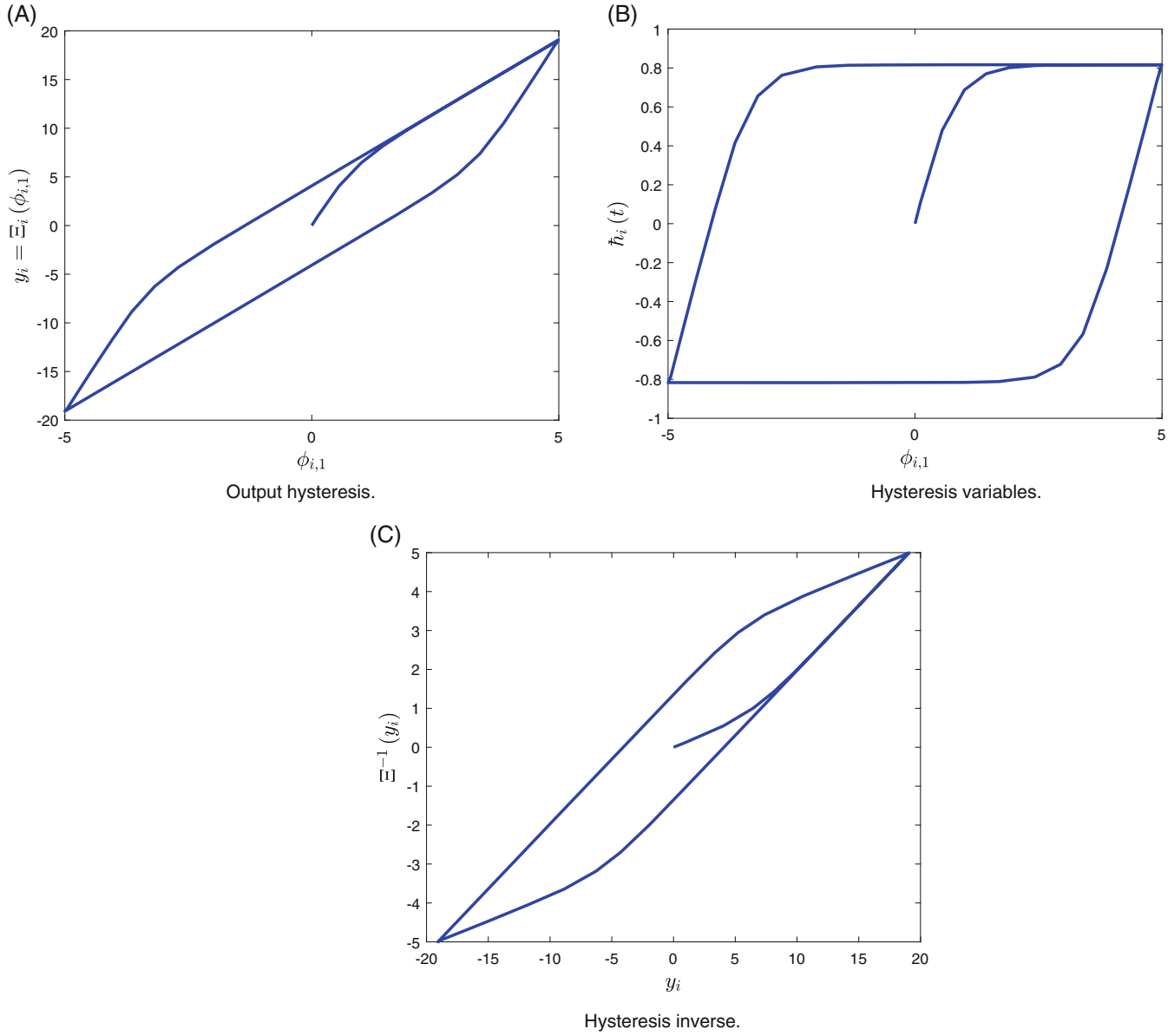

FIGURE 2 Output hysteresis structure

Lemma 1 (41). *Supposing $\Lambda_i(t)$ and $\eta_i(t)$ are smooth functions defined in $[0, t_f]$, then $\Lambda_i(t)$, $\eta_i(t)$ and $\int_0^{t_f}(\psi_i(t)N_i(\eta_i)+1)\dot{\eta}_i e^{-\Theta_{i,2}(t-\tau)}d\tau$ are all bounded for $t \in [0, t_f]$ and $t_f < +\infty$, if the following inequalities hold*

$$0 \le \Lambda_i(t) \le \Theta_{i,1} + \int_0^{t_f}(\psi_i N_i(\eta_i)+1)\dot{\eta}_i e^{-\Theta_{i,2}(t-\tau)}d\tau, \tag{16}$$

where $\psi_i(t)$ are the time-varying coefficients with value on $E_i := [\Upsilon_i^-, \Upsilon_i^+]$ and $0 \notin E_i$, $N_i(\eta_i)$ are smooth Nussbaum-type functions, and $\Theta_{i,1}, \Theta_{i,2}$ are positive scalars.

2.5 | Multi-dimensional Taylor network

MTN is an especial three layer NN, and its structure is shown in Figure 3. In this article, the MTN is introduced into the controller design process to handle with the unknown nonlinearity. For MTN, the following Lemma holds.

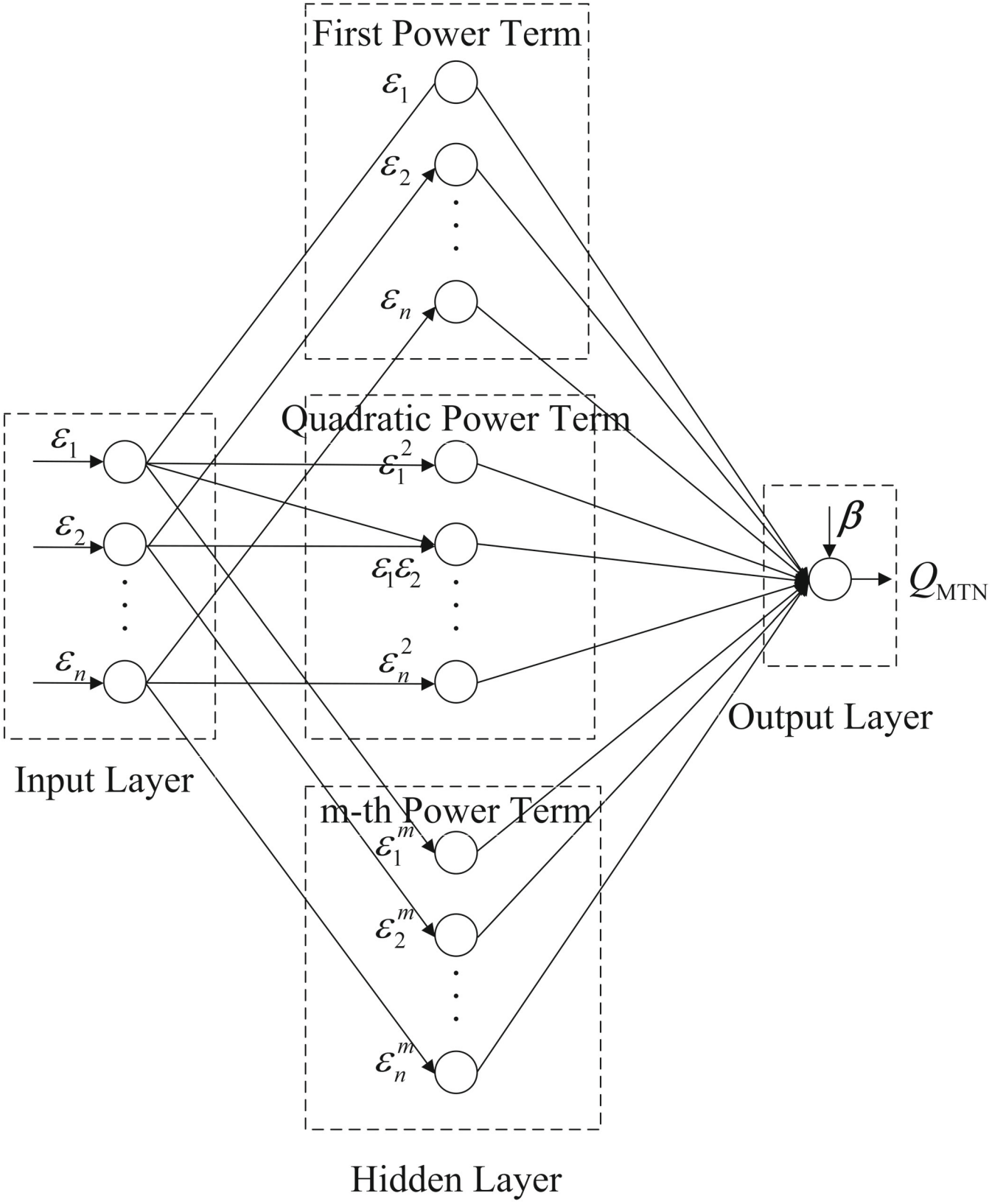

FIGURE 3 Topological structure of MTN

Lemma 2 (10). *On a compact set Ω, for a continuous function $Q(\boldsymbol{\varepsilon}) : R^n \to R$, and $\forall\sigma > 0$, there exists a MTN $\boldsymbol{\beta}^{\mathrm{T}} P_{m_n}(\boldsymbol{\varepsilon})$ as follow*

$$Q(\boldsymbol{\varepsilon}) = \boldsymbol{\beta}^{*\mathrm{T}} P_{m_n}(\boldsymbol{\varepsilon}) + \delta(\boldsymbol{\varepsilon}), \tag{17}$$

where $P_{m_n}(\boldsymbol{\varepsilon}) \triangleq \left[\varepsilon_1, \ldots, \varepsilon_n, \varepsilon_1^2, \ldots, \varepsilon_n^2, \ldots, \varepsilon_1^m, \ldots, \varepsilon_n^m\right]^{\mathrm{T}} \in R^l$ is the middle layer vector of MTN. $\boldsymbol{\varepsilon} \triangleq [\varepsilon_1, \varepsilon_2, \ldots, \varepsilon_n]^{\mathrm{T}} \in R^n$ is the input vector of MTN. $\delta(\boldsymbol{\varepsilon})$ is the approximate error between $Q(\boldsymbol{\varepsilon})$ and $\boldsymbol{\beta}^{\mathrm{T}} P_{m_n}(\boldsymbol{\varepsilon})$, and $|\delta(\boldsymbol{\varepsilon})| < \sigma$. $\boldsymbol{\beta}$ is the weight vector of MTN, and $\boldsymbol{\beta}^* := \arg\min_{\beta \in R^l} \left\{ \sup_{\Lambda \in \Omega} \left| Q(\boldsymbol{\varepsilon}) - \boldsymbol{\beta}^{\mathrm{T}} P_{m_n}(\boldsymbol{\varepsilon}) \right| \right\} \in R^l$.

3 | ADAPTIVE MTN TRACKING CONTROLLER DESIGN

Firstly, defining the coordinate transformation as follows

$$\begin{cases} z_{i,1} = y_i - y_{i,d} \\ z_{i,j} = \phi_{i,j} - \alpha_{i,j-1}, j = 2, \ldots, n_i \end{cases}, \tag{18}$$

where $i = 1, \ldots, N$, $y_{i,d}$ are the reference signals. $\alpha_{i,j-1}$ are the virtual control signals, which values will be given in later design.

Secondly, for $i = 1, 2, \ldots, N, j = 1, 2, \ldots, n_i$, unknown constants $\beta_{i,j}$ are defined, and $\beta_{i,j} = \max\left\{ \left\| \boldsymbol{\beta}_{i,j,k} \right\|^2 : k \in M \right\}$. $\boldsymbol{\beta}_{i,j,k}$ are the weight vectors of MTN, and their values will be given later. $\hat{\beta}_{i,j}$ are the estimated values of $\beta_{i,j}$ and satisfy $\tilde{\beta}_{i,j} = \beta_{i,j} - \hat{\beta}_{i,j}$.

Step i, 1: Constructing the 1th Lyapunov functions as follows

$$V_{i,1} = \frac{1}{2} z_{i,1}^2 + \frac{1}{2} \tilde{\beta}_{i,1}^2. \tag{19}$$

Based on $z_{i,1} = y_i - y_{i,d}$, (1) and (19), the time derivative of $V_{i,1}$ are as follows

$$\dot{V}_{i,1} = \kappa_i(t) z_{i,1} \left(z_{i,2} + \alpha_{i,1} + \gamma_{i,1,k} + \Delta_{i,1,k} + A_{i,1,k}(\bar{\boldsymbol{y}}) \right) - z_{i,1} \dot{y}_{i,d} - \tilde{\beta}_{i,1} \dot{\hat{\beta}}_{i,1}. \tag{20}$$

With the help of Young's inequality, and taking Assumptions 2 and 3 into consideration, the following inequalities can be obtained.

$$\kappa_i(t) z_{i,1} z_{i,2} \le \frac{\overline{\kappa}_i^2}{2} z_{i,1}^2 + \frac{1}{2} z_{i,2}^2, \tag{21}$$

$$\kappa_i(t) z_{i,1} A_{i,1,k}(\bar{\boldsymbol{y}}) \le \frac{\overline{\kappa}_i}{2} z_{i,1}^2 + \frac{1}{2} A_{i,1,k}^2(\bar{\boldsymbol{y}}) \le \frac{\overline{\kappa}_i}{2} z_{i,1}^2 + \frac{1}{2} \sum_{l=1}^{N} y_l^2 \tilde{A}_{i,1,k,l}^2(y_l), \tag{22}$$

$$z_{i,1} \kappa_i(t) \left(\gamma_{i,1,k} + \Delta_{i,1,k} \right) \le \frac{1}{2} a_{i,1}^2 + \frac{\overline{\kappa}_i^2}{2 a_{i,1}^2} z_{i,1}^2 R_{i,1,k}^2 \tag{23}$$

with $R_{i,1,k} = \gamma_{i,1,k} + \varphi_{i,1,k}\left(t, \bar{\boldsymbol{\phi}}_{i,1}\right) + \tilde{\varphi}_{i,1,k}$ are continuous functions, and $a_{i,1} > 0$ are constants.

Then, from (20), (21), (22), and (23), the time derivative of $V_{i,1}$ can be redescribed in the following form.

$$\dot{V}_{i,1} \le -2 w_{i,1} z_{i,1}^2 + \frac{1}{2} z_{i,2}^2 + \frac{1}{2} a_{i,1}^2 + z_{i,1} \left[\kappa_i(t) \alpha_{i,1} + Q_{i,1,k} \right] + \frac{1}{2} \sum_{l=1}^{N} y_l^2 \tilde{A}_{i,1,k,l}^2(y_l) - B_i\left(z_{i,1}^2\right) z_{i,1}^2 - \tilde{\beta}_{i,1} \dot{\hat{\beta}}_{i,1}, \tag{24}$$

where $Q_{i,1,k} = \frac{\overline{\kappa}_i^2}{2 a_{i,1}^2} z_{i,1} R_{i,1,k}^2 - \dot{y}_{i,d} + \left(2 w_{i,1} + \overline{\kappa}_i^2\right) z_{i,1} + B_i\left(z_{i,1}^2\right) z_{i,1}$ are unknown functions. $B_i\left(z_{i,1}^2\right)$ indicate auxiliary functions. $w_{i,1} > 0$ are constants.

For unknown functions $Q_{i,1,k}$, in the light of Lemma 2, for $\forall \sigma_{i,1,k} > 0$, there must be a MTN can be used to approximate them, in other words, $Q_{i,1,k}$ satisfy

$$Q_{i,1,k} = \boldsymbol{\beta}_{i,1,k}^{\mathrm{T}} P_{m_{i,1}}\left(\overline{\boldsymbol{\phi}}_{i,1}\right) + \delta_{i,1,k}\left(\overline{\boldsymbol{\phi}}_{i,1}\right) \tag{25}$$

with $\overline{\boldsymbol{\phi}}_{i,1} = \left[\phi_{i,1}\right]^{\mathrm{T}}$, $\delta_{i,1,k}\left(\overline{\boldsymbol{\phi}}_{i,1}\right)$ are the error between $Q_{i,1,k}$ and $\boldsymbol{\beta}_{i,1,k}^{\mathrm{T}} P_{m_{i,1}}\left(\overline{\boldsymbol{\phi}}_{i,1}\right)$.

From Young's inequality and (25), the following inequalities can be acquired.

$$\begin{aligned} z_{i,1}Q_{i,1,k} &\le \frac{1}{2}\ell_{i,1}^2 + \frac{1}{2\ell_{i,1}^2} z_{i,1}^2 \left\|\boldsymbol{\beta}_{i,1,k}\right\|^2 P_{m_{i,1}}^{\mathrm{T}} P_{m_{i,1}} + \frac{1}{2} z_{i,1}^2 + \frac{1}{2}\sigma_{i,1,k}^2 \\ &\le \frac{1}{2}\ell_{i,1}^2 + \frac{1}{2\ell_{i,1}^2} z_{i,1}^2 \beta_{i,1} P_{m_{i,1}}^{\mathrm{T}} P_{m_{i,1}} + \frac{1}{2} z_{i,1}^2 + \frac{1}{2}\sigma_{i,1,k}^2 \end{aligned} \tag{26}$$

with $\ell_{i,1} > 0$ denote constants.

Then, comprehensive consideration of (24) and (26), the virtual control signals $\alpha_{i,1}$ can be designed as follows

$$\alpha_{i,1} = N_i\left(\eta_i\right)\left[-\left(w_{i,1} + \frac{1}{2}\right) z_{i,1} + \frac{1}{2\ell_{i,1}^2} z_{i,1}\hat{\beta}_{i,1} P_{m_{i,1}}^{\mathrm{T}} P_{m_{i,1}}\right]. \tag{27}$$

Combining (24), (26), and (27), one has

$$\begin{aligned} \dot{V}_{i,1} \le &-\left(w_{i,1} - 1\right) z_{i,1}^2 + \left[\kappa_i(t) N_i\left(\eta_i\right) + 1\right]\dot{\eta}_i + \tilde{\beta}_{i,1}\left(\frac{1}{2\ell_{i,1}^2} z_{i,1}^2 P_{m_{i,1}}^{\mathrm{T}} P_{m_{i,1}} - \dot{\hat{\beta}}_{i,1}\right) \\ &+ \frac{1}{2}\left(a_{i,1}^2 + \ell_{i,1}^2 + \sigma_{i,1,k}^2\right) + \frac{1}{2}\sum_{l=1}^{N} y_l^2 \tilde{A}_{i,1,k,l}^2\left(y_l\right) - B_i\left(z_{i,1}^2\right) z_{i,1}^2 + \frac{1}{2} z_{i,2}^2 \end{aligned} \tag{28}$$

with the adaptive laws can be design as $\dot{\eta}_i = -\left(w_{i,1} + \frac{1}{2}\right) z_{i,1}^2 + \frac{1}{2\ell_{i,1}^2} z_{i,1}^2 \hat{\beta}_{i,1} P_{m_{i,1}}^{\mathrm{T}} P_{m_{i,1}}$.

Step i, 2: Constructing the 2nd Lyapunov functions as follows

$$V_{i,2} = V_{i,1} + \frac{1}{2} z_{i,2}^2 + \frac{1}{2}\tilde{\beta}_{i,2}^2. \tag{29}$$

Based on $z_{i,2} = \phi_{i,2} - \alpha_{i,1}$, (1) and (29), the time derivative of $V_{i,2}$ are as follows

$$\dot{V}_{i,2} = z_{i,2}\left(z_{i,3} + \alpha_{i,2} + \gamma_{i,2,k} + \Delta_{i,2,k} + A_{i,2,k}(\overline{\boldsymbol{y}}) - \dot{\alpha}_{i,1}\right) - \tilde{\beta}_{i,2}\dot{\hat{\beta}}_{i,2} + \dot{V}_{i,1} \tag{30}$$

with $i = 1, 2, \ldots, N$, $\dot{\alpha}_{i,1} = \frac{\partial \alpha_{i,1}}{\partial \hat{\beta}_{i,1}}\dot{\hat{\beta}}_{i,1} + \frac{\partial \alpha_{i,1}}{\partial \phi_{i,1}}\dot{\phi}_{i,1} + \frac{\partial \alpha_{i,1}}{\partial y_i}\dot{y}_i + \frac{\partial \alpha_{i,1}}{\partial \eta_i}\dot{\eta}_i + \sum_{l=0}^{1}\frac{\partial \alpha_{i,1}}{\partial y_{i,d}} y_{i,d}^{(l+1)}$.

By the aid of Young's inequality, taking Assumptions 2 and 3, the following inequalities can be gained.

$$z_{i,2} z_{i,3} \le \frac{1}{2} z_{i,2}^2 + \frac{1}{2} z_{i,3}^2, \tag{31}$$

$$z_{i,2} A_{i,2,k}(\overline{\boldsymbol{y}}) \le \frac{1}{2} z_{i,2}^2 + \frac{1}{2} A_{i,2,k}^2(\overline{\boldsymbol{y}}) \le \frac{1}{2} z_{i,2}^2 + \frac{1}{2}\sum_{l=1}^{N} y_l^2 \tilde{A}_{i,2,k,l}^2\left(y_l\right), \tag{32}$$

$$z_{i,2}\left(\gamma_{i,2,k} + \Delta_{i,2,k}\right) \le \frac{1}{2} a_{i,2}^2 + \frac{1}{2a_{i,2}^2} z_{i,2}^2 R_{i,2,k}^2 \tag{33}$$

with $R_{i,2,k} = \gamma_{i,2,k} + \varphi_{i,2,k}\left(t, \overline{\boldsymbol{\phi}}_{i,2}\right) + \tilde{\varphi}_{i,2,k}$ are continuous functions, and $a_{i,2} > 0$ are constants.

Then, from (30), (31), (32), and (33), it follows that

$$\dot{V}_{i,2} \leq \dot{V}_{i,1} + z_{i,2}^2 + \frac{1}{2}z_{i,3}^2 + \frac{1}{2}a_{i,2}^2 + z_{i,2}\left(\alpha_{i,2} + Q_{i,2,k}\right) + \frac{1}{2}\sum_{l=1}^{N} y_l^2 \tilde{A}_{i,2,k,l}^2\left(y_l\right) - \tilde{\beta}_{i,2}\dot{\hat{\beta}}_{i,2} \tag{34}$$

with $Q_{i,2,k} = \frac{1}{2a_{i,2}^2} z_{i,2} R_{i,2,k}^2 - \dot{\alpha}_{i,1}$ are unknown functions.

For unknown functions $Q_{i,2,k}$, in the light of Lemma 2, for $\forall \sigma_{i,2,k} > 0$, there must be a MTN can be used to approximate them, in other words, $Q_{i,2,k}$ satisfy

$$Q_{i,2,k} = \boldsymbol{\beta}_{i,2,k}^{\mathrm{T}} P_{m_{i,2}}\left(\overline{\boldsymbol{\phi}}_{i,2}\right) + \delta_{i,2,k}\left(\overline{\boldsymbol{\phi}}_{i,2}\right) \tag{35}$$

with $\overline{\boldsymbol{\phi}}_{i,2} = \left[\phi_{i,1}, \phi_{i,2}\right]^{\mathrm{T}}$, $\delta_{i,2,k}$ are the error between $Q_{i,2,k}$ and $\boldsymbol{\beta}_{i,2,k}^{\mathrm{T}} P_{m_{i,2}}\left(\overline{\boldsymbol{\phi}}_{i,2}\right)$.

Based on (35) and with the help of Young's inequality, the following inequalities are true.

$$\begin{aligned} z_{i,2}Q_{i,2,k} &\leq \frac{1}{2}\ell_{i,2}^2 + \frac{1}{2\ell_{i,2}^2} z_{i,2}^2 \left\|\boldsymbol{\beta}_{i,2,k}\right\|^2 P_{m_{i,2}}^{\mathrm{T}} P_{m_{i,2}} + \frac{1}{2}z_{i,2}^2 + \frac{1}{2}\sigma_{i,2,k}^2 \\ &\leq \frac{1}{2}\ell_{i,2}^2 + \frac{1}{2\ell_{i,2}^2} z_{i,2}^2 \beta_{i,2} P_{m_{i,2}}^{\mathrm{T}} P_{m_{i,2}} + \frac{1}{2}z_{i,2}^2 + \frac{1}{2}\sigma_{i,2,k}^2 \end{aligned} \tag{36}$$

with $\ell_{i,2} > 0$ denote constants.

Then, comprehensive consideration of (34) and (36), the virtual control signals $\alpha_{i,2}$ can be designed as follows

$$\alpha_{i,2} = -\left(w_{i,2} + 1\right) z_{i,2} - \frac{1}{2\ell_{i,2}^2} z_{i,2} \hat{\beta}_{i,2} P_{m_{i,2}}^{\mathrm{T}} P_{m_{i,2}} \tag{37}$$

with $w_{i,2} > 0$ are constants.

Combining (28), (34), (36), and (37), the new form of $\dot{V}_{i,2}$ can be expressed as

$$\begin{aligned} \dot{V}_{i,2} \leq &-\sum_{q=1}^{2}\left(w_{i,q} - 1\right) z_{i,q}^2 + \left[\kappa_i(t) N_i\left(\eta_i\right) + 1\right]\dot{\eta}_i + \sum_{q=1}^{2}\tilde{\beta}_{i,q}\left(\frac{1}{2\ell_{i,q}^2} z_{i,q}^2 P_{m_{i,q}}^{\mathrm{T}} P_{m_{i,q}} - \dot{\hat{\beta}}_{i,q}\right) \\ &+ \frac{1}{2}\sum_{q=1}^{2}\left(a_{i,q}^2 + \ell_{i,q}^2 + \sigma_{i,q,k}^2\right) + \frac{1}{2}\sum_{q=1}^{2}\sum_{l=1}^{N} y_l^2 \tilde{A}_{i,q,k,l}^2\left(y_l\right) - B_i\left(z_{i,1}^2\right) z_{i,1}^2 + \frac{1}{2}z_{i,3}^2. \end{aligned} \tag{38}$$

Step $i, j\ (3 \leq j \leq n_i - 1)$: Constructing the jth Lyapunov functions as follows

$$V_{i,j} = V_{i,j-1} + \frac{1}{2}z_{i,j}^2 + \frac{1}{2}\tilde{\beta}_{i,j}^2. \tag{39}$$

Based on $z_{i,j} = \phi_{i,j} - \alpha_{i,j-1}$, (1) and (39), the time derivative of $V_{i,j}$ are as follows

$$\dot{V}_{i,j} = z_{i,j}\left(z_{i,j+1} + \alpha_{i,j} + \gamma_{i,j,k} + \Delta_{i,j,k} + A_{i,j,k}(\overline{\mathbf{y}}) - \dot{\alpha}_{i,j-1}\right) - \tilde{\beta}_{i,j}\dot{\hat{\beta}}_{i,j} + \dot{V}_{i,j-1} \tag{40}$$

with $i = 1, 2, \ldots, N, j = 2, \ldots, n_i - 2$, $\dot{\alpha}_{i,j} = \sum_{l=1}^{j} \frac{\partial \alpha_{i,j}}{\partial \hat{\beta}_{i,l}}\dot{\hat{\beta}}_{i,l} + \sum_{l=1}^{j} \frac{\partial \alpha_{i,j}}{\partial \phi_{i,l}}\dot{\phi}_{i,l} + \frac{\partial \alpha_{i,j}}{\partial y_i}\dot{y}_i + \frac{\partial \alpha_{i,j}}{\partial \eta_i}\dot{\eta}_i + \sum_{l=0}^{j} \frac{\partial \alpha_{i,j}}{\partial y_{i,d}} y_{i,d}^{(l+1)}$.

On the basis of Young's inequality, taking Assumptions 2 and 3 into consideration, the following inequalities can be achieved.

$$z_{i,j}z_{i,j+1} \leq \frac{1}{2}z_{i,j}^2 + \frac{1}{2}z_{i,j+1}^2, \tag{41}$$

$$z_{i,j}A_{i,j,k}(\overline{\mathbf{y}}) \leq \frac{1}{2}z_{i,j}^2 + \frac{1}{2}A_{i,j,k}^2(\overline{\mathbf{y}}) \leq \frac{1}{2}z_{i,j}^2 + \frac{1}{2}\sum_{l=1}^{N} y_l^2 \tilde{A}_{i,j,k,l}^2\left(y_l\right), \tag{42}$$

$$z_{i,j}\left(\gamma_{i,j,k}+\Delta_{i,j,k}\right)\leq\frac{1}{2}a_{i,j}^{2}+\frac{1}{2a_{i,j}^{2}}z_{i,j}^{2}R_{i,j,k}^{2} \tag{43}$$

with $R_{i,j,k}=\gamma_{i,j,k}+\varphi_{i,j,k}\left(t,\overline{\boldsymbol{\phi}}_{i,j}\right)+\tilde{\varphi}_{i,j,k}$ are continuous functions, and $a_{i,j}>0$ are constants.

Then, from (40), (41), (42), and (43), it follows that

$$\dot{V}_{i,j}\leq z_{i,j}^{2}+\frac{1}{2}z_{i,j+1}^{2}+\frac{1}{2}a_{i,j}^{2}+z_{i,j}\left(\alpha_{i,j}+Q_{i,j,k}\right)+\frac{1}{2}\sum_{l=1}^{N}y_{l}^{2}\tilde{A}_{i,j,k,l}^{2}\left(y_{l}\right)-\tilde{\beta}_{i,j}\dot{\hat{\beta}}_{i,j}+\dot{V}_{i,j-1} \tag{44}$$

with $Q_{i,j,k}=\frac{1}{2a_{i,j}^{2}}z_{i,j}R_{i,j,k}^{2}-\dot{\alpha}_{i,j-1}$ are unknown functions.

For unknown functions $Q_{i,j,k}$, in the light of Lemma 2, for $\forall\sigma_{i,j,k}>0$, there must be a MTN can be used to approximate them, in other words, $Q_{i,j,k}$ satisfy

$$Q_{i,j,k}=\boldsymbol{\beta}_{i,j,k}^{\mathrm{T}}P_{m_{i,j}}\left(\overline{\boldsymbol{\phi}}_{i,j}\right)+\delta_{i,j,k}\left(\overline{\boldsymbol{\phi}}_{i,j}\right) \tag{45}$$

with $\overline{\boldsymbol{\phi}}_{i,j}=\left[\phi_{i,1},\ \ldots\ ,\phi_{i,j}\right]^{\mathrm{T}}$, $\delta_{i,j,k}$ are the error between $Q_{i,j,k}$ and $\boldsymbol{\beta}_{i,j,k}^{\mathrm{T}}P_{m_{i,j}}\left(\overline{\boldsymbol{\phi}}_{i,j}\right)$.

Based on (45) and with the help of Young's inequality, the following inequalities are true.

$$\begin{aligned}z_{i,j}Q_{i,j,k}&\leq\frac{1}{2}\ell_{i,j}^{2}+\frac{1}{2\ell_{i,j}^{2}}z_{i,j}^{2}\left\|\boldsymbol{\beta}_{i,j,k}\right\|^{2}P_{m_{i,j}}^{\mathrm{T}}P_{m_{i,j}}+\frac{1}{2}z_{i,j}^{2}+\frac{1}{2}\sigma_{i,j,k}^{2}\\&\leq\frac{1}{2}\ell_{i,j}^{2}+\frac{1}{2\ell_{i,j}^{2}}z_{i,j}^{2}\beta_{i,j}P_{m_{i,j}}^{\mathrm{T}}P_{m_{i,j}}+\frac{1}{2}z_{i,j}^{2}+\frac{1}{2}\sigma_{i,j,k}^{2}\end{aligned} \tag{46}$$

with $\ell_{i,j}>0$ denote constants.

Then, comprehensive consideration of (44) and (46), the virtual control signals $\alpha_{i,j}$ can be designed as follows

$$\alpha_{i,j}=-\left(w_{i,j}+1\right)z_{i,j}-\frac{1}{2\ell_{i,j}^{2}}z_{i,j}\hat{\beta}_{i,j}P_{m_{i,j}}^{\mathrm{T}}P_{m_{i,j}} \tag{47}$$

with $w_{i,j}>0$ are constants.

Combining (44), (46), (47) and repeating Step $i,2$, the new form of $\dot{V}_{i,j}$ can be described as

$$\begin{aligned}\dot{V}_{i,j}\leq&-\sum_{q=1}^{j}\left(w_{i,q}-1\right)z_{i,q}^{2}+\left[\kappa_{i}(t)N_{i}\left(\eta_{i}\right)+1\right]\dot{\eta}_{i}+\sum_{q=1}^{j}\tilde{\beta}_{i,q}\left(\frac{1}{2\ell_{i,q}^{2}}z_{i,q}^{2}P_{m_{i,q}}^{\mathrm{T}}P_{m_{i,q}}-\dot{\hat{\beta}}_{i,q}\right)\\&+\frac{1}{2}\sum_{q=1}^{j}\left(a_{i,q}^{2}+\ell_{i,q}^{2}+\sigma_{i,q,k}^{2}\right)+\frac{1}{2}\sum_{q=1}^{j}\sum_{l=1}^{N}y_{l}^{2}\tilde{A}_{i,q,k,l}^{2}\left(y_{l}\right)-B_{i}\left(z_{i,1}^{2}\right)z_{i,1}^{2}+\frac{1}{2}z_{i,j+1}^{2}.\end{aligned} \tag{48}$$

Remark 4. Term $\frac{1}{2}z_{i,j+1}^{2}$, $i=1,2,n,j=1,2,n_{i}-1$ will be solved in the Step $i,j+1$.

Step i,n_i: Constructing the n_ith Lyapunov functions as follows

$$V_{i,n_{i}}=V_{i,n_{i}-1}+\frac{1}{2}z_{i,n_{i}}^{2}+\frac{1}{2}\tilde{\beta}_{i,n_{i}}^{2}. \tag{49}$$

Based on $z_{i,n_i}=\phi_{i,n_i}-\alpha_{i,n_i-1}$, (1) and (49), the time derivative of V_{i,n_i} are as follows

$$\dot{V}_{i,n_{i}}=z_{i,n_{i}}\left(\chi_{i}^{\prime}v_{i}+c_{i}+\gamma_{i,n_{i},k}+\Delta_{i,n_{i},k}+A_{i,n_{i},k}(\overline{\boldsymbol{y}})-\dot{\alpha}_{i,n_{i}-1}\right)-\tilde{\beta}_{i,n_{i}}\dot{\hat{\beta}}_{i,n_{i}}+\dot{V}_{i,n_{i}-1} \tag{50}$$

with $i=1,2,\ \ldots\ ,N$, $\dot{\alpha}_{i,n_i-1}=\sum_{l=1}^{n_i-1}\frac{\partial\alpha_{i,n_i-1}}{\partial\hat{\beta}_{i,l}}\dot{\hat{\beta}}_{i,l}+\sum_{l=1}^{n_i-1}\frac{\partial\alpha_{i,n_i-1}}{\partial\phi_{i,l}}\dot{\phi}_{i,l}+\frac{\partial\alpha_{i,1}}{\partial y_i}\dot{y}_i+\frac{\partial\alpha_{i,1}}{\partial\eta_i}\dot{\eta}_i+\sum_{l=0}^{n_i-1}\frac{\partial\alpha_{i,n_i-1}}{\partial y_{i,d}}y_{i,d}^{(l+1)}$.

By the aid of Young's inequality, taking Assumptions 2 and 3 into consideration, the following inequalities can be gained.

$$z_{i,n_i}A_{i,n_i,k}(\overline{\boldsymbol{y}}) \le \frac{1}{2}z_{i,n_i}^2 + \frac{1}{2}A_{i,n_i,k}^2(\overline{\boldsymbol{y}}) \le \frac{1}{2}z_{i,n_i}^2 + \frac{1}{2}\sum_{l=1}^{N} y_l^2\tilde{A}_{i,n_i,k,l}^2(y_l), \tag{51}$$

$$z_{i,n_i}c_i \le \frac{1}{2}z_{i,n_i}^2 + \frac{1}{2}\bar{c}_i^2, \tag{52}$$

$$z_{i,n_i}\left(\gamma_{i,n_i,k} + \Delta_{i,n_i,k}\right) \le \frac{1}{2}a_{i,n_i}^2 + \frac{1}{2a_{i,n_i}^2}z_{i,n_i}^2R_{i,n_i,k}^2 \tag{53}$$

with $R_{i,n_i,k} = \gamma_{i,n_i,k} + \varphi_{i,n_i,k}\left(t, \overline{\boldsymbol{\phi}}_{i,n_i}\right) + \tilde{\varphi}_{i,n_i,k}$ are continuous functions, and $a_{i,n_i} > 0$ are constants.

Then, from (50), (51), (52), and (53), it follows that

$$\dot{V}_{i,n_i} = \dot{V}_{i,n_i-1} + z_{i,n_i}^2 + \frac{1}{2}\bar{c}_i + \frac{1}{2}a_{i,n_i}^2 + z_{i,n_i}\left(\chi_i'v_i + Q_{i,n_i,k}\right) + \frac{1}{2}\sum_{l=1}^{N} y_l^2\tilde{A}_{i,n_i,k,l}^2(y_l) - \tilde{\beta}_{i,n_i}\dot{\hat{\beta}}_{i,n_i} \tag{54}$$

with $Q_{i,n_i,k} = \frac{1}{2a_{i,n_i}^2}z_{i,n_i}R_{i,n_i,k}^2 - \dot{\alpha}_{i,n_i-1}$ are unknown functions.

For unknown functions $Q_{i,n_i,k}$, on the basis of Lemma 2, for $\forall\sigma_{i,n_i,k} > 0$, there must be a MTN can be used to approximate them, in other words, $Q_{i,n_i,k}$ satisfy

$$Q_{i,n_i,k} = \boldsymbol{\beta}_{i,n_i,k}^{\mathrm{T}}P_{m_{i,n_i}}\left(\overline{\boldsymbol{\phi}}_{i,n_i}\right) + \delta_{i,n_i,k}\left(\overline{\boldsymbol{\phi}}_{i,n_i}\right) \tag{55}$$

with $\overline{\boldsymbol{\phi}}_{i,n_i} = \left[\phi_{i,1}, \phi_{i,2}, \ldots, \phi_{i,n_i}\right]^{\mathrm{T}}$, $\delta_{i,n_i,k}$ are the error between $Q_{i,n_i,k}$ and $\boldsymbol{\beta}_{i,n_i,k}^{\mathrm{T}}P_{m_{i,n_i}}\left(\overline{\boldsymbol{\phi}}_{i,n_i}\right)$.

Based on (55) and with the help of Young's inequality, the following inequalities are true.

$$\begin{aligned} z_{i,n_i}Q_{i,n_i,k} &\le \frac{1}{2}\ell_{i,n_i}^2 + \frac{1}{2\ell_{i,n_i}^2}z_{i,n_i}^2\left\|\boldsymbol{\beta}_{i,n_i,k}\right\|^2P_{m_{i,n_i}}^{\mathrm{T}}P_{m_{i,n_i}} + \frac{1}{2}z_{i,n_i}^2 + \frac{1}{2}\sigma_{i,n_i,k}^2 \\ &\le \frac{1}{2}\ell_{i,n_i}^2 + \frac{1}{2\ell_{i,n_i}^2}z_{i,n_i}^2\beta_{i,n_i}P_{m_{i,n_i}}^{\mathrm{T}}P_{m_{i,n_i}} + \frac{1}{2}z_{i,n_i}^2 + \frac{1}{2}\sigma_{i,n_i,k}^2 \end{aligned} \tag{56}$$

with $\ell_{i,n_i} > 0$ denote constants.

Then, comprehensive consideration of (54) and (56), the control inputs v_i can be designed as follows

$$v_i = -\frac{1}{k}\left[\left(w_{i,n_i} + 1\right)z_{i,n_i} + \frac{1}{2\ell_{i,n_i}^2}z_{i,n_i}\hat{\beta}_{i,n_i}P_{m_{i,n_i}}^{\mathrm{T}}P_{m_{i,n_i}}\right] \tag{57}$$

with $w_{i,n_i} > 0$ are constants.

Combining Assumption 4, (48), (54), (56), and (57), the new form of $\dot{V}_{i,n_i}$ can be described as

$$\begin{aligned} \dot{V}_{i,n_i} \le &-\sum_{q=1}^{n_i} r_{i,q}z_{i,q}^2 + \left[\kappa_i(t)N_i(\eta_i) + 1\right]\dot{\eta}_i + \sum_{q=1}^{n_i}\tilde{\beta}_{i,q}\left(\frac{1}{2\ell_{i,q}^2}z_{i,q}^2P_{m_{i,q}}^{\mathrm{T}}P_{m_{i,q}} - \dot{\hat{\beta}}_{i,q}\right) \\ &+ \frac{1}{2}\sum_{q=1}^{n_i}\left(a_{i,q}^2 + \ell_{i,q}^2 + \sigma_{i,q,k}^2\right) + \frac{1}{2}\bar{c}_i^2 + \frac{1}{2}\sum_{q=1}^{n_i}\sum_{l=1}^{N} y_l^2\tilde{A}_{i,q,k,l}^2(y_l) - B_i\left(z_{i,1}^2\right)z_{i,1}^2, \end{aligned} \tag{58}$$

where $r_{i,q} = w_{i,q} - 1 > 0$.

4 | STABILITY ANALYSIS

Theorem 1. *Considering large-scale switched nonlinear systems (1) subject to asymmetric input saturation and unknown output hysteresis, if the virtual control signals and the control inputs are designed as (27), (37), (47) and (57), the adaptive*

control laws are designed as

$$\dot{\hat{\beta}}_{i,j} = -\xi_{i,j}\hat{\beta}_{i,j} + \frac{1}{2\ell_{i,j}^2} z_{i,j}^2 P_{m_{i,j}}^{\mathrm{T}} P_{m_{i,j}}, \tag{59}$$

where $i = 1, \ldots, N, j = 1, \ldots, n_i, \xi_{i,j} > 0$ *are constants. For any bounded initial conditions, one has*

(i) For the closed-loop system, all signals in it are bounded;
(ii) Tracking error $y_i - y_{i,d}$ *can converge to an adjustable region of the origin.*

Proof. Based on Section 3, constructing the Lyapunov function for the closed-loop system as follows

$$V = \frac{1}{2}\sum_{i=1}^{N}\sum_{j=1}^{n_i} z_{i,j}^2 + \frac{1}{2}\sum_{i=1}^{N}\sum_{j=1}^{n_i} \tilde{\beta}_{i,j}^2. \tag{60}$$

Then, it follows from (58) that

$$\begin{aligned}\dot{V} \le & -\sum_{i=1}^{N}\sum_{j=1}^{n_i} r_{i,j} z_{i,j}^2 + \sum_{i=1}^{N}\left[\kappa_i(t) N_i(\eta_i) + 1\right]\dot{\eta}_i + \frac{1}{2}\sum_{i=1}^{N}\sum_{j=1}^{n_i}\left(a_{i,j}^2 + \ell_{i,j}^2 + \sigma_{i,j,k}^2\right) + \frac{1}{2}\sum_{i=1}^{N}\bar{c}_i^2 \\ & + \sum_{i=1}^{N}\sum_{j=1}^{n_i}\tilde{\beta}_{i,j}\left(\frac{1}{2\ell_{i,j}^2} z_{i,j}^2 P_{m_{i,j}}^{\mathrm{T}} P_{m_{i,j}} - \dot{\hat{\beta}}_{i,j}\right) + \frac{1}{2}\sum_{i=1}^{N}\sum_{j=1}^{n_i}\sum_{l=1}^{N} y_l^2 \tilde{A}_{i,j,k,l}^2(y_l) - \sum_{i=1}^{N} B_i\left(z_{i,1}^2\right) z_{i,1}^2.\end{aligned} \tag{61}$$

According to (59), the following inequalities can be derived.

$$\tilde{\beta}_{i,j}\left(\frac{1}{2\ell_{i,j}^2} z_{i,j}^2 P_{m_{i,j}}^{\mathrm{T}} P_{m_{i,j}} - \dot{\hat{\beta}}_{i,j}\right) \le -\frac{1}{2}\xi_{i,j}\tilde{\beta}_{i,j}^2 + \frac{1}{2}\xi_{i,j}\beta_{i,j}^2. \tag{62}$$

In addition, the following inequality is ensured by selecting the appropriate auxiliary functions $B_i\left(z_{i,1}^2\right)$.

$$\frac{1}{2}\sum_{i=1}^{N}\sum_{j=1}^{n_i}\sum_{l=1}^{N} y_l^2 \tilde{A}_{i,j,k,l}^2(y_l) - \sum_{i=1}^{N} B_i\left(z_{i,1}^2\right) z_{i,1}^2 \le 0. \tag{63}$$

From (61), (62), and (63), it follows that

$$\dot{V} \le -aV + b + \sum_{i=1}^{N}\left[\kappa_i(t) N_i(\eta_i) + 1\right]\dot{\eta}_i \tag{64}$$

where for $k \in M, i = 1, \ldots, N, j = 1, \ldots, n_i$, $a = \min\left\{2r_{i,j}, \xi_{i,j}\right\}$, $b = \frac{1}{2}\sum_{i=1}^{N}\sum_{j=1}^{n_i}\xi_{i,j}\beta_{i,j}^2 + \frac{1}{2}\sum_{i=1}^{N}\sum_{j=1}^{n_i}\left(a_{i,j}^2 + \ell_{i,j}^2 + \sigma_{i,j,\max}^2\right) + \frac{1}{2}\sum_{i=1}^{N}\bar{c}_i^2$, $\sigma_{i,j,\max}^2 = \max\left\{\sigma_{i,j,k}^2 | k \in M\right\}$.

Integrating (64) from 0 to t $(t > 0)$, the following inequality holds

$$0 \le V \le \left[V(0) - \frac{b}{a}\right] e^{-at} + \frac{b}{a} + e^{-at}\sum_{i=1}^{N}\int_0^t \left[\kappa_i(t) N_i(\eta_i) + 1\right]\dot{\eta}_i e^{a\tau} d\tau. \tag{65}$$

Similar to Reference 41, according to inequality (65), the conclusion can be drawn that all signals of the closed-loop system are bounded, and the tracking error can be adjusted to a small neighborhood of the origin.

That completes the proof of Theorem 1. ∎

5 | SIMULATION STUDY

The effectiveness of the proposed controller is verified by a numerical example and a practical example.

Example 1. Considering the following large-scale switched nonlinear system subject to asymmetric input saturation and output hysteresis.

$$\begin{cases} \dot{\phi}_{1,1} = \phi_{1,2} + \gamma_{1,1,k}\left(\overline{\boldsymbol{\phi}}_{1,1}\right) + \Delta_{1,1,k}\left(t, \overline{\boldsymbol{\phi}}_{1,1}\right) + A_{1,1,k}(\overline{\boldsymbol{y}}) \\ \dot{\phi}_{1,2} = u_1\left(v_1(t)\right) + \gamma_{1,2,k}\left(\overline{\boldsymbol{\phi}}_{1,2}\right) + \Delta_{1,2,k}\left(t, \overline{\boldsymbol{\phi}}_{1,2}\right) + A_{1,2,k}(\overline{\boldsymbol{y}}) \\ y_1 = p_{1,1}\phi_{1,1} + p_{1,2}\hbar_1 \\ \dot{\phi}_{2,1} = \phi_{2,2} + \gamma_{2,1,k}\left(\overline{\boldsymbol{\phi}}_{2,1}\right) + \Delta_{2,1,k}\left(t, \overline{\boldsymbol{\phi}}_{2,1}\right) + A_{2,1,k}(\overline{\boldsymbol{y}}) \\ \dot{\phi}_{2,2} = u_2\left(v_2(t)\right) + \gamma_{2,2,k}\left(\overline{\boldsymbol{\phi}}_{2,2}\right) + \Delta_{2,2,k}\left(t, \overline{\boldsymbol{\phi}}_{2,2}\right) + A_{2,2,k}(\overline{\boldsymbol{y}}) \\ y_2 = p_{2,1}\phi_{2,1} + p_{2,2}\hbar_2 \end{cases} \tag{66}$$

with initial states $\phi_{1,1}(0) = \phi_{1,2}(0) = \phi_{2,1}(0) = \phi_{2,2}(0) = 0$. For $\forall k \in M$, $\sigma(t) : [0, \infty) \to M = \{1, 2\}$ is the switching signal. When $k = 1$, the nonlinear functions in the system are set as $\gamma_{1,1,1} = -0.2\phi_{1,1}$, $\gamma_{1,2,1} = -0.2\phi_{1,1}\phi_{1,2}$, $\gamma_{2,1,1} = -0.2\phi_{2,1}$, $\gamma_{2,2,1} = -0.2\phi_{2,1}\phi_{2,2}$, $\Delta_{1,1,1} = \phi_{1,1}\sin\pi t$, $\Delta_{1,2,1} = \phi_{1,2}^2\sin\pi t$, $\Delta_{2,1,1} = \phi_{2,1}\sin\pi t$, $\Delta_{2,2,1} = \phi_{2,1}\phi_{2,2}\sin\pi t$, $A_{1,1,1} = y_1y_2$, $A_{1,2,1} = y_1^2y_2$, $A_{2,1,1} = y_1y_2$, $A_{2,2,1} = y_1y_2^2$. When $k = 2$, the nonlinear functions in the system are set as $\gamma_{1,1,2} = -0.1\phi_{1,1}^2$, $\gamma_{1,2,2} = -0.1\phi_{1,2}^2$, $\gamma_{2,1,2} = -0.1\phi_{2,1}^2$, $\gamma_{2,2,2} = -0.1\phi_{2,2}^2$, $\Delta_{1,1,2} = \phi_{1,1}\cos\pi t$, $\Delta_{1,2,2} = \phi_{1,1}\phi_{1,2}\cos\pi t$, $\Delta_{2,1,2} = \phi_{2,1}\cos\pi t$, $\Delta_{2,2,2} = \phi_{2,1}\phi_{2,2}\cos\pi t$, $A_{1,1,2} = 0.5y_1y_2$, $A_{1,2,2} = 0.5y_1^2y_2$, $A_{2,1,2} = 0.5y_1y_2$, $A_{2,2,2} = 0.5y_1y_2^2$.

For $i, j = 1, 2$, the parameters settings of output hysteresis are as follows: $p_{i,j} = 1$, $\iota_i = 5$, $K_i = 2$, $\lambda_i = 3.5$. Therefore, the output hysteresis can be expressed as $y_i = \phi_{i,1} + \hbar_i$, with $\begin{cases} \dot{\hbar}_i = \dot{\phi}_{i,1} - 5\left|\dot{\phi}_{i,1}\right|\left|\hbar_i\right|\hbar_i - 3.5\dot{\phi}_{i,1}|\hbar_i|^2 \\ \hbar_i(t_0) = 0 \end{cases}$.

According to Theorem 1, the control structures of system (66) can be designed as follows.

$$\begin{aligned} \alpha_{i,1} &= N_i(\eta_i)\left[-\left(w_{i,1} + \frac{1}{2}\right)z_{i,1} + \frac{1}{2\ell_{i,1}^2}z_{i,1}\hat{\beta}_{i,1}P_{m_{i,1}}^{\mathrm{T}}P_{m_{i,1}}\right], \\ v_i &= -\frac{1}{k}\left[\left(w_{i,2} + 1\right)z_{i,2} + \frac{1}{2\ell_{i,2}^2}z_{i,2}\hat{\beta}_{i,2}P_{m_{i,2}}^{\mathrm{T}}P_{m_{i,2}}\right], \\ \dot{\hat{\beta}}_{i,j} &= -\xi_{i,j}\hat{\beta}_{i,j} + \frac{1}{2\ell_{i,j}^2}z_{i,j}^2P_{m_{i,j}}^{\mathrm{T}}P_{m_{i,j}} \end{aligned} \tag{67}$$

with $i, j = 1, 2$, $N_i(\eta_i) = \eta_i^2\cos\eta_i$, $\dot{\eta}_i = -\left(w_{i,1} + \frac{1}{2}\right)z_{i,1}^2 + \frac{1}{2\ell_{i,1}^2}z_{i,1}^2\hat{\beta}_{i,1}P_{m_{i,1}}^{\mathrm{T}}P_{m_{i,1}}$, $z_{i,1} = \phi_{i,1} - y_{i,d}$, $z_{i,2} = \phi_{i,2} - \alpha_{i,1}$, $\boldsymbol{z}_{i,1} = \left[z_{i,1}\right]^{\mathrm{T}}$, $\boldsymbol{z}_{i,2} = \left[z_{i,1}, z_{i,2}\right]^{\mathrm{T}}$. The parameters of the design controller are as follows: $k = 1$, $w_{1,1} = 159.5$, $w_{1,2} = 29$, $w_{2,1} = 129.5$, $w_{2,2} = 89$, $\xi_{1,1} = 1$, $\xi_{1,2} = 2$, $\xi_{2,1} = 0.1$, $\xi_{2,2} = 0.2$, $\ell_{1,1} = \ell_{1,2} = \ell_{2,1} = \ell_{2,2} = 1$, $u_{1,\max} = 8$, $u_{1,\min} = 9$, $u_{2,\max} = 40$, $u_{2,\min} = 10$. The simulation results are shown in Figures 4–8.

The trajectories of the system output $y_i(t)$ and their reference signals $y_{i,d}(t)$ are shown in Figure 4. The asymmetric control inputs $v_i(t)$ are displayed in Figure 5. Figures 6–8 respectively reveal the state variables $\phi_{1,2}$, $\phi_{2,2}$, switching signal $\sigma(t)$ and the tracking error of the system (66). The tracking error can converge to an adjustable region of the origin. It can be concluded from the simulation results in Figures 4–8 that the control strategy proposed in this article is effective.

Example 2. The inverted pendulum connected by two springs is controlled to verify the effectiveness of the control scheme proposed in this article, which can be transformed as a switched nonlinear system.[42]

$$\begin{cases} \dot{\phi}_{i,1} = \phi_{i,2} \\ \dot{\phi}_{i,2} = u_i\left(v_i(t)\right) + \left(\frac{m_igl}{J} - \frac{Sr^2}{4J}\right)\sin\left(\phi_{i,1}\right) + \frac{Sr(l-b)}{2J} + \gamma_{i,2,k}\left(\overline{\boldsymbol{\phi}}_{i,2}\right) + A_{i,2,k}(\overline{\boldsymbol{y}}), \\ y_i = p_{i,1}\phi_{i,1} + p_{i,2}\hbar_i \end{cases} \tag{68}$$

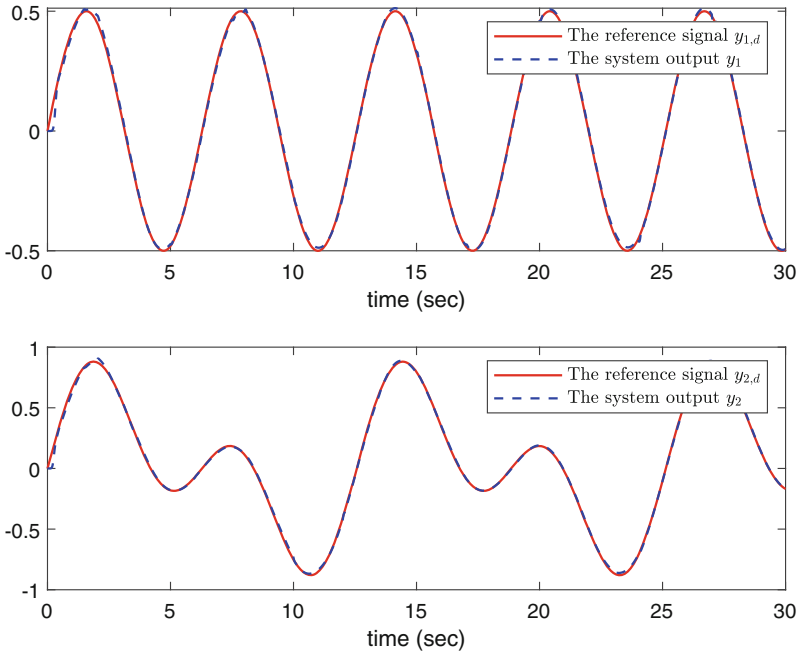

FIGURE 4 System output $y_i(t)$ and reference signal $y_{i,d}(t)$ of Example 1

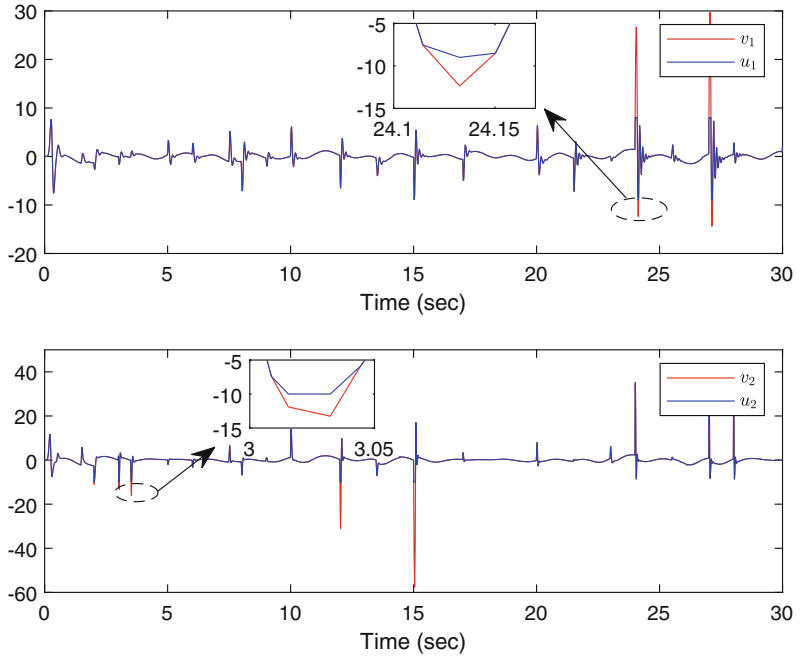

FIGURE 5 System control input of Example 1

where $i = 1, 2$ and the initial states, switching signal, the parameters setting of output hysteresis, and the control structures of system are the same as those in Example 1. When $k = 1$, the nonlinear functions in the system are set as $\gamma_{1,2,1} = \frac{\phi_{1,1}\sin(\phi_{1,1}\phi_{1,2})}{m_1}$, $\gamma_{2,2,1} = \frac{\phi_{2,1}\sin(\phi_{2,1}\phi_{2,2})}{m_2}$, $A_{1,2,1} = \frac{Sr^2}{4J}\sin(y_1)$, $A_{2,2,1} = \frac{Sr^2}{4J}\sin(y_2)$. When $k = 2$, the nonlinear functions in the system are set as $\gamma_{1,2,2} = \frac{\phi_{1,2}\cos(\phi_{1,1})}{m_1}$, $\gamma_{2,2,2} = \frac{\phi_{2,2}\cos(\phi_{2,2})}{m_2}$, $A_{1,2,2} = A_{2,2,2} = \frac{Sr^2}{4J}\sin(y_1y_2)$. The parameters design of the inverted pendulum connected by two springs are shown in the Table 1. The parameters of the design controller are as

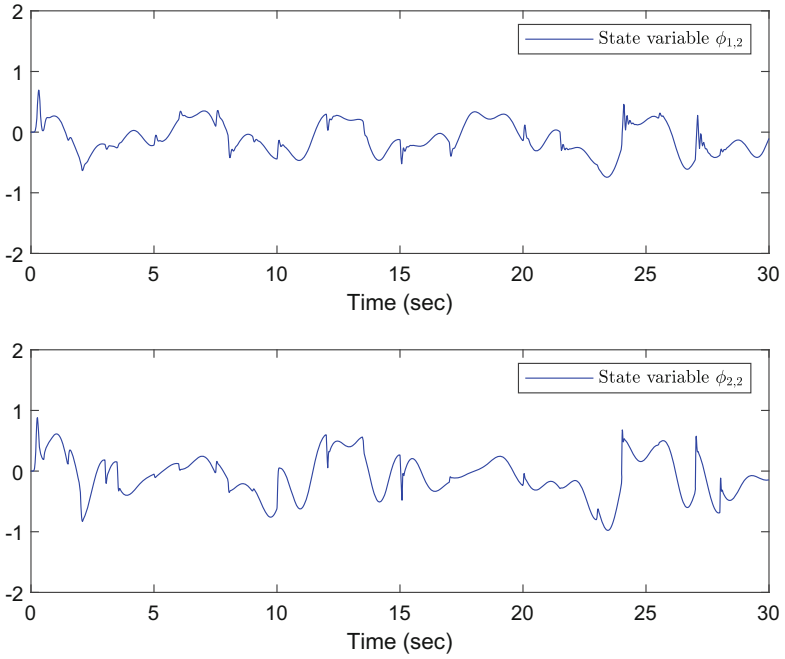

FIGURE 6 State variables $\phi_{1,2}, \phi_{2,2}$ of Example 1

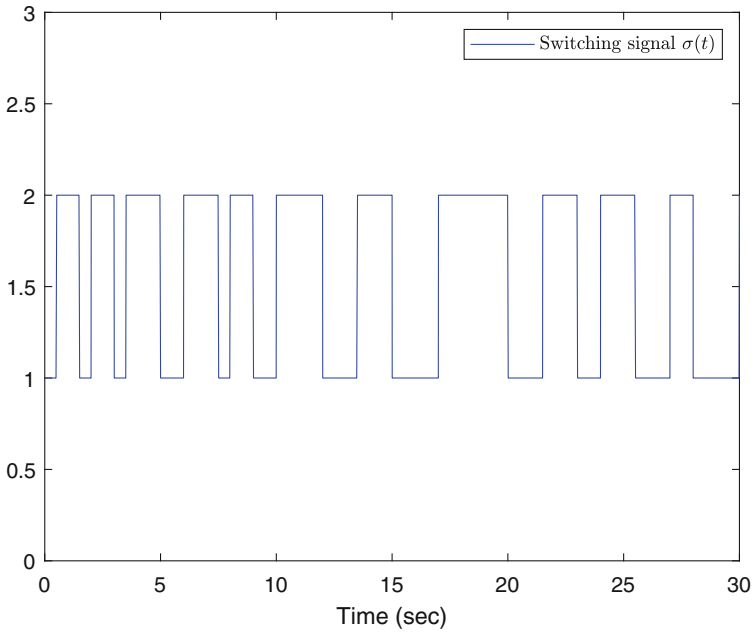

FIGURE 7 Switching signal of Example 1

follows: $k = 1, w_{1,1} = 99.5, w_{1,2} = 9, w_{2,1} = 99.5, w_{2,2} = 49, \xi_{1,1} = 1, \xi_{1,2} = 2, \xi_{2,1} = 0.1, \xi_{2,2} = 0.2, \ell_{1,1} = \ell_{1,2} = \ell_{2,1} = \ell_{2,2} = 1$, $u_{1,\max} = 5$, $u_{1,\min} = 4$, $u_{2,\max} = 7$, $u_{2,\min} = 8$. The simulation results are shown in Figures 9–13.

Figures 9–13 show that the control strategy proposed in this article can still achieve good results for practical system. The above results further prove the effectiveness of the proposed controller.

Remark 5. In view of the following three aspects, the complexity of the adaptive MTN control strategy proposed in this article is effectively reduced. (i) On the basis of backstepping technology, the construction of Lyapunov functions and the controller design process are procedural, which ensures that the control strategy proposed in

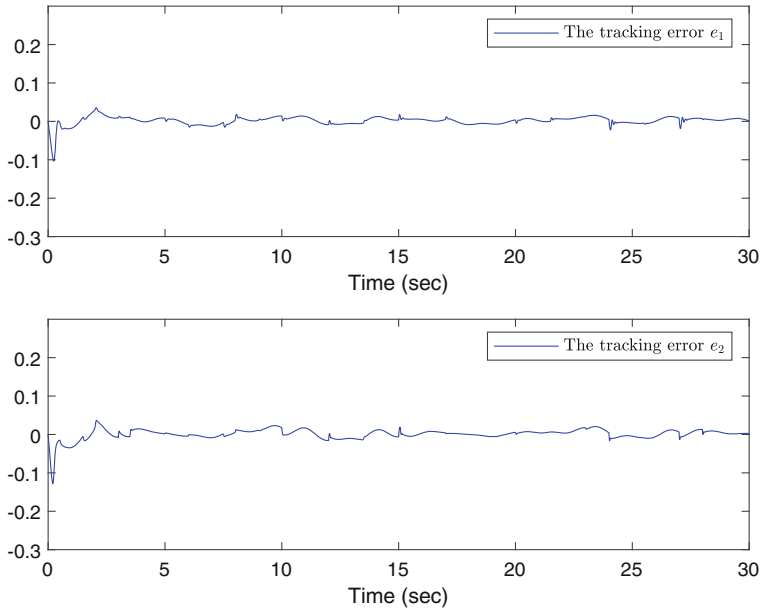

FIGURE 8 The tracking error of Example 1

TABLE 1 The parameters of system (68)

Parameter name	Parameter value
Pendulum end masses m_1, m_2	0.1 kg, 0.2 kg
Moments of inertia J	1 kg
Spring constant S	10 N/m
The height of pendulum r	0.5 m
The spring's natural length l	0.5 m
Gravitational acceleration g	9.8 m/s^2
The distance between two pendulum hinges b	0.4 m

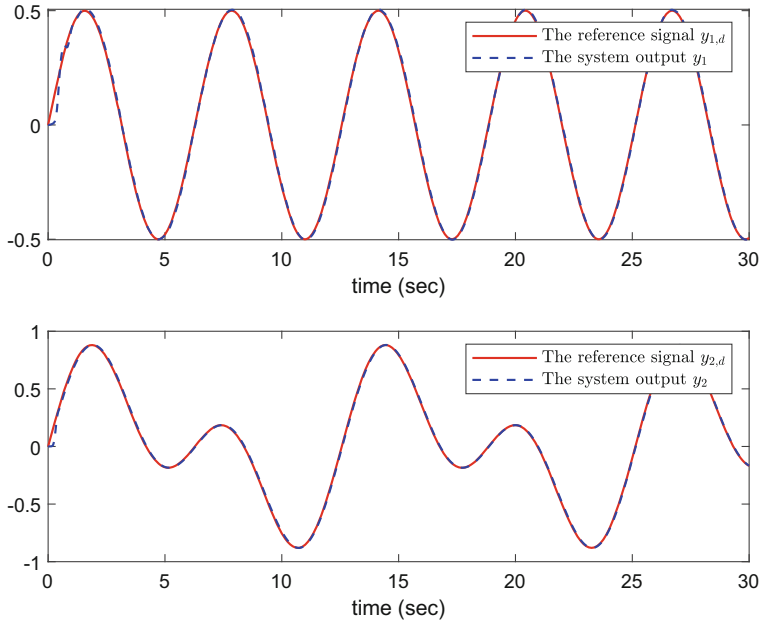

FIGURE 9 System output $y_i(t)$ and reference signal $y_{i,d}(t)$ of Example 2

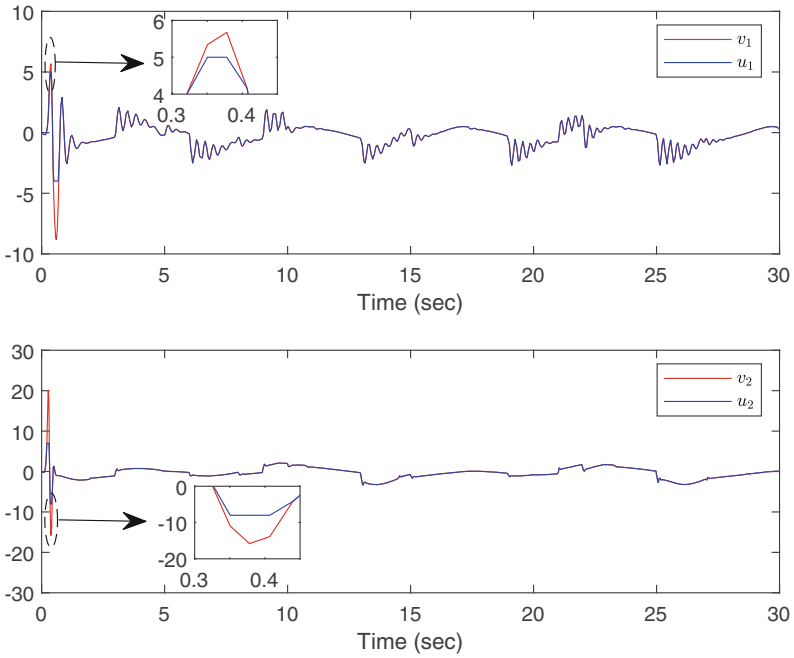

FIGURE 10 System control input of Example 2

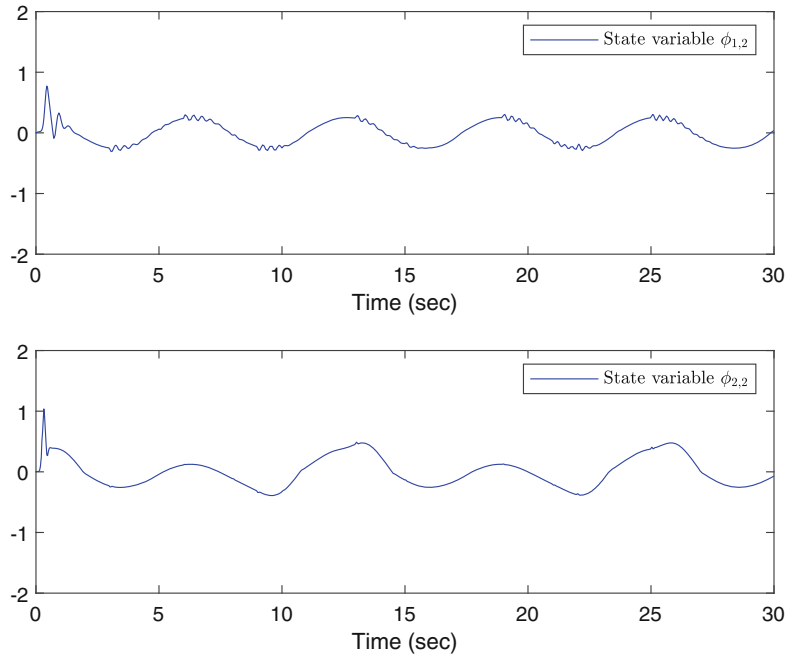

FIGURE 11 State variables $\phi_{1,2}, \phi_{2,2}$ of Example 2

this article is easy to achieve. (ii) Either in comparison to large-scale nonlinear systems[27,28] or switched nonlinear systems[29] with asymmetric input saturation constraints, or in comparison to switched nonlinear systems with output hysteresis,[39] this article investigates the control problem of more general large-scale switched nonlinear systems, and the proposed controller structures are simpler. (iii) As a kind of NN with special structure, MTN adopts polynomial to approximate nonlinearity, which greatly reduces the computational complexity. The MTN-based control strategy is easy to be applied in practice, which has excellent dynamic performance and can realizes real-time tracking.

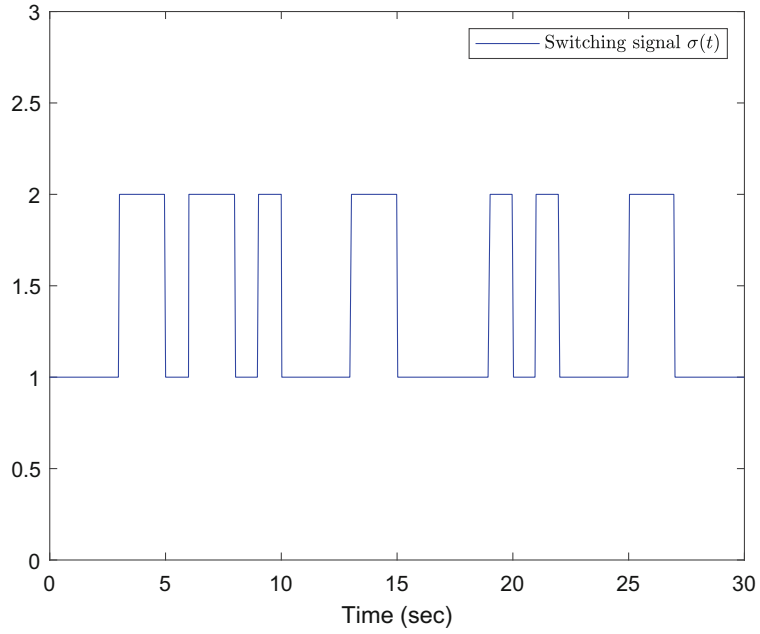

FIGURE 12 Switching signal of Example 2

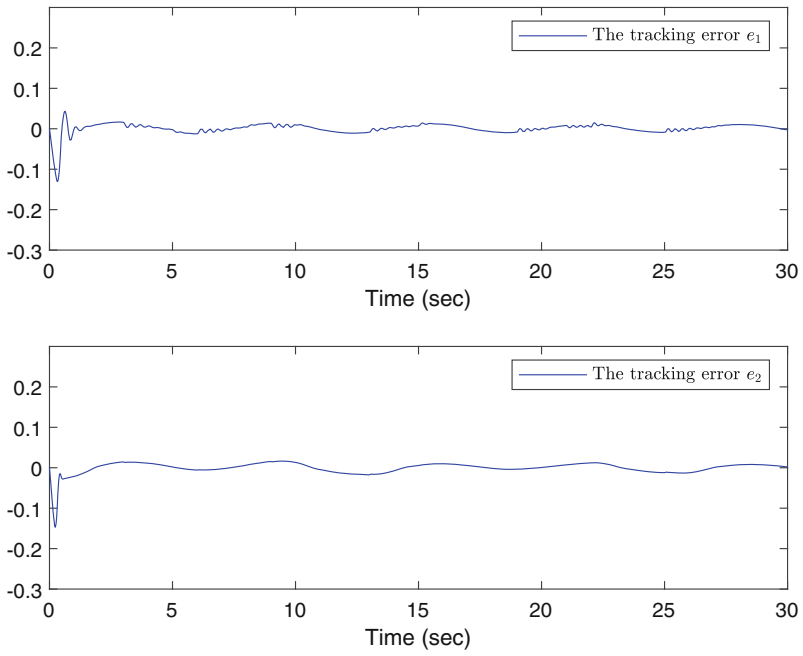

FIGURE 13 The tracking error of Example 2

6 | CONCLUSION

The problem of tracking control for large-scale switched nonlinear systems with asymmetric input saturation constraint and output hysteresis is studied in this article. Firstly, the asymmetric input saturation constraint in the controlled system is transformed into the combination of a linear function and a bounded error function. Secondly, the nonlinear output hysteresis in the controlled system is converted into a linear problem. Thirdly, in the control process, an adaptive backstepping control strategy based on common Lyapunov functions is proposed by combining Nussbaum function with MTN technology. Significantly, it is the first time that asymmetric input saturation constraint and output hysteresis are

considered for large-scale switched systems. Finally, two simulation examples are given to verify the effectiveness of the control scheme proposed in this article.

FUNDING INFORMATION

Shandong Provincial Natural Science Foundation, China (No. ZR2020QF055).

ORCID

Yu-Qun Han https://orcid.org/0000-0002-9055-2954
Wen-Jing He https://orcid.org/0000-0001-6370-592X
Na Li https://orcid.org/0000-0002-7911-8903

REFERENCES

1. Cui Q, Huang JS, Gao TT. Adaptive leaderless consensus control of uncertain multiagent systems with unknown control directions. *Int J Robust Nonlinear Control*. 2020;30(15):6229-6240.
2. Niu B, Zhao P, Liu JD, Ma HJ, Liu YJ. Global adaptive control of switched uncertain nonlinear systems: An improved MDADT method. *Automatica*. 2020;115:108872.
3. Wu ZH, Guo BZ. Active disturbance rejection control to MIMO nonlinear systems with stochastic uncertainties: approximate decoupling and output-feedback stabilisation. *Int J Control*. 2020;93(6):1408-1427.
4. Tong SC, Min X, Li YX. Observer-based adaptive fuzzy tracking control for strict-feedback nonlinear systems with unknown control gain functions. *IEEE Trans Cybern*. 2020;50(9):3903-3913.
5. Ma JL, Xu SY, Zhuang GM, Wei YL, Zhang ZQ. Adaptive neural network tracking control for uncertain nonlinear systems with input delay and saturation. *Int J Robust Nonlinear Control*. 2020;30(7):2593-2610.
6. Sun W, Su SF, Wu YQ, Xia JW. Novel adaptive fuzzy control for output constrained stochastic nonstrict feedback nonlinear systems. *IEEE Trans Fuzzy Syst*. 2021;29(5):1188-1197.
7. Liu YJ, Chen CLP, Wen GX, Tong SC. Adaptive neural output feedback tracking control for a class of uncertain discrete-time nonlinear systems. *IEEE Trans Neural Netw*. 2011;22(7):1162-1167.
8. Han YQ, Zhu SL, Yang SG, Chu L. Adaptive multi-dimensional Taylor network tracking control for a class of nonlinear systems. *Int J Control*. 2021;94(2):277-285.
9. Han YQ, Yan HS. Observer-based multi-dimensional Taylor network decentralised adaptive tracking control of large-scale stochastic nonlinear systems. *Int J Control*. 2020;93(7):1605-1618.
10. Han YQ. Design of decentralized adaptive control approach for large-scale nonlinear systems subjected to input delays under prescribed performance. *Nonlinear Dyn*. 2021;106(1):565-582.
11. He WJ, Han YQ, Li N, Zhu SL. Novel adaptive controller design for a class of switched nonlinear systems subject to input delay using multi-dimensional Taylor network. *Int J Adapt Control Signal Process*. 2022;36(3):607-624.
12. He WJ, Zhu SL, Li N, Han YQ. Adaptive controller design for switched stochastic nonlinear systems subject to unknown dead-zone input via new type of network approach. *Int J Control Autom Syst*. 2022; (Accepted).
13. Li N, Han YQ, He WJ, Zhu SL. Control design for stochastic nonlinear systems with full-state constraints and input delay: a new adaptive approximation method. *Int J Control Autom Syst*. 2021; (Accepted).
14. Zhang JJ, Yan HS. MTN optimal control of MIMO non-affine nonlinear time-varying discrete systems for tracking only by output feedback. *J Franklin Inst*. 2019;356(8):4304-4334.
15. Zhao X, Yuan SF, Zhou HB, Sun HB, Qiu L. An evaluation on the multi-agent system based structural health monitoring for large scale structures. *Expert Syst Appl*. 2009;36(3):4900-4914.
16. Wells BE, Ricks KG, Weir JM. Parallel simulation of a large-scale aerospace system in a multicomputer environment. *IEEE Trans Aerosp Electron Syst*. 1997;33(2):507-522.
17. Guo Y, Hill DJ, Wang YY. Nonlinear decentralized control of large-scale power systems. *Automatica*. 2000;36(9):1275-1289.
18. Sui S, Tong SC, Chen CLP. Finite-time filter decentralized control for nonstrict-feedback nonlinear large-scale systems. *IEEE Trans Fuzzy Syst*. 2018;26(6):3289-3300.
19. Liu X, Zhai D. Adaptive decentralized control for switched nonlinear large-scale systems with quantized input signal. *Nonlinear Anal Hybrid Syst*. 2020;35:100817.
20. Liu SJ, Zhang JF, Jiang ZP. Decentralized adaptive output-feedback stabilization for large-scale stochastic nonlinear systems. *Automatica*. 2007;43(2):238-251.
21. Itoh A, Takahashi W, Nagano H, Kurisaka M, Iwasaki S. Practical implementation and packaging technologies for a large-scale ATM switching system. *IEEE J Select Areas Commun*. 1991;9(8):1280-1288.
22. Villumsen JC, Brønmo G, Philpott AB. Line capacity expansion and transmission switching in power systems with large-scale wind power. *IEEE Trans Power Syst*. 2013;28(2):731-739.
23. Li YM, Tong SC. Fuzzy adaptive control design strategy of nonlinear switched large-scale systems. *IEEE Trans Syst Man Cybern Syst*. 2018;48(12):2209-2218.

24. Tong SC, Zhang LL, Li YM. Observed-based adaptive fuzzy decentralized tracking control for switched uncertain nonlinear large-scale systems with dead zones. *IEEE Trans Syst Man Cybern Syst*. 2016;46(1):37-47.
25. Ye BH, Long LJ, Zhao J. Adaptive dynamic surface control of switched MIMO nonlinear systems with input saturation and its application to NSVs. *Asian J Control*. 2020;22(6):2363-2376.
26. Chang R, Fang YM, Liu L, Li JX. Decentralized prescribed performance adaptive tracking control for Markovian jump uncertain nonlinear systems with input saturation. *Int J Adapt Control Signal Process*. 2017;31(2):255-274.
27. Zhu SL, Han YQ. Adaptive decentralized prescribed performance control for a class of large-scale nonlinear systems subject to nonsymmetric input saturations. *Neural Comput Appl*. 2022;34(13):11123-11140.
28. Si WJ. Approximation-based decentralized output-feedback control for uncertain stochastic interconnected nonlinear time-delay systems with input delay and asymmetric input saturation. *J Franklin Inst*. 2018;355(15):7098-7133.
29. Zhang WH, Wei W. Disturbance-observer-based finite-time adaptive fuzzy control for non-triangular switched nonlinear systems with input saturation. *Inform Sci*. 2021;561:152-167.
30. Lai ZL, Nagarajaiah S. Sparse structural system identification method for nonlinear dynamic systems with hysteresis/inelastic behavior. *Mech Syst Signal Process*. 2019;117:813-842.
31. Huang XY, Zhang H, Zhang GG, Wang JM. Robust weighted gain-scheduling H∞ vehicle lateral motion control with considerations of steering system backlash-type hysteresis. *IEEE Trans Control Syst Technol*. 2014;22(5):1740-1753.
32. Chen XK, Su CY, Fukuda T. Adaptive control for the systems preceded by hysteresis. *IEEE Trans Automat Contr*. 2008;53(4):1019-1025.
33. Tao G, Kokotovic PV. Adaptive control of plants with unknown hystereses. *IEEE Trans Automat Contr*. 1995;40(2):200-212.
34. Macki JW, Nistri P, Zecca P. Mathematical models for hysteresis. *SIAM Rev*. 1993;35(1):94-123.
35. Zhou J, Wen CY, Li TS. Adaptive output feedback control of uncertain nonlinear systems with hysteresis nonlinearity. *IEEE Trans Automat Contr*. 2012;57(10):2627-2633.
36. Wu LB, Wang H, He XQ, Zhang DQ. Decentralized adaptive fuzzy tracking control for a class of uncertain large-scale systems with actuator nonlinearities. *Appl Math Comput*. 2018;332:390-405.
37. Namadchian Z, Rouhani M. Adaptive neural tracking control of switched stochastic pure-feedback nonlinear systems with unknown Bouc-Wen hysteresis input. *IEEE Trans Neural Netw Learn Syst*. 2018;29(12):5859-5869.
38. Ma L, Huo X, Zhao XD, Niu B, Zong GD. Adaptive neural control for switched nonlinear systems with unknown backlash-like hysteresis and output dead-zone. *Neurocomputing*. 2019;357:203-214.
39. He WJ, Zhu SL, Li N, Han YQ. Tracking control for switched nonlinear systems subject to output hysteresis via adaptive multi-dimensional Taylor network approach. *Int J Control*. 2022. doi:10.1080/00207179.2022.2067787
40. Lyu ZL, Liu Z, Zhang Y, Chen CLP. Adaptive neural control for switched nonlinear systems with unmodeled dynamics and unknown output hysteresis. *Neurocomputing*. 2019;341:107-117.
41. Liu Z, Lai GY, Zhang Y, Chen CLP. Adaptive neural output feedback control of output-constrained nonlinear systems with unknown output nonlinearity. *IEEE Trans Neural Netw Learn Syst*. 2015;26(8):1789-1802.
42. Zhang LL, Yang GH. Adaptive fuzzy output constrained decentralized control for switched nonlinear large-scale systems with unknown dead zones. *Nonlinear Anal Hybrid Syst*. 2017;23:61-75.

How to cite this article: Han Y-Q, He W-J, Li N, Zhu S-L. Tracking control for large-scale switched nonlinear systems subject to asymmetric input saturation and output hysteresis: A new adaptive network-based approach. *Int J Robust Nonlinear Control*. 2022;32(14):8052-8072. doi: 10.1002/rnc.6258